

Reply to reviewer #1 comments:

Thank you very much for agreeing to review this paper and for your comments that have permitted to improve the quality of the manuscript.

Most of your comments have been taken into account in the revised version of the manuscript and all the proposed references have been added.

Please find below a point-by-point reply relative to your comments.

From the first part of the abstract, it seems that the neodymium isotopic composition of both mixed planktonic foraminifera and cold-water corals (CWC) have been investigated at the three selected locations. This could be made clear since CWC have been analyzed only at the Alboran Sea and the south Sardinian continental margin and foraminifera only at the Balearic basin. This aspect could be clarified, also explaining how the data have been integrated. The abstract includes the main implications of the study for hydrological variations during the deposition of the S1 sapropel but the data are also relevant to the deposition of the ORL1.

The abstract has been revised in order to make clear the different archives and locations of the study. We have also added a sentence to explain how the data have been integrated. However, the deposition of the ORL1 being not the aim of this paper, we do not conclude on potential implications about it.

The introduction could better highlight the aim of the work. Moreover, the classical references on Mediterranean climate variability are cited but more recent ones could also be included, for instance Martrat et al (2014) provide interesting high-resolution data on surface water variability of the Mediterranean Sea during the last two deglaciations, including the Holocene.

The introduction has been sharpened up following your recommendations and those of the reviewer #2. Martrat et al. (2014) has not been added in the introduction as we do not think that discussing SST variability in the introduction is relevant in our paper. However, this reference has been cited in other parts of the text.

In the material and methods section, though references are provided to get detailed information about CWC cores, additional information on core description could also be included in this paper to facilitate the whole picture of the analyzed materials. Similarly, a new core recovered in the Balearic Sea has been investigated but little is said about the description of the materials sampled except for barren of any CWC fragments. It is also mentioned that samples from this core have been used for multiproxy analyses but other than dating and estimation of SST by modern analogue techniques only neodymium and stable isotopes been analyzed so this could be better specified in section 3.1.

Additional information on the CWC and SU92.33 cores have now been included in the text. The term “multiproxy analyses” has been replaced by “ $\delta^{18}\text{O}$, $\delta^{13}\text{C}$ and ϵNd analyzes”.

Regarding the results section, there are three different subsections on core SU92- 33 that may be omitted and the results could be synthesized in just one as for CWC.

The subsections have been deleted and the results have been synthesized in two sections: CWC and core SU-92.33

Some general sentences referred to sedimentation rate as “the lowest values observed during the Holocene” could be more specific.

The sentence has been modified in order to better quantify the sedimentation rate.

In this section the information concerning the core MD90-917 is insufficient, it is cited as a well dated record but it is not clear if the references cited in the paragraph (line 294) are those providing the data included in Fig. 2a (in which a reference is not cited).

The reference for this core (Siani et al., 2004) has been integrated in the paragraph.

The discussion is relevant and highlights the most important aspects of the hydrological variations in the Mediterranean. However, some aspects could be further discussed as the role of the eolian input in the ϵNd variability and why it is not affected by changes in such input. Concerning this, some additional papers on eolian input could be considered, for instance Scheuven et al. (2013) on bulk composition of northern African dust or Rodrigo-Gamiz et al (2015) on terrigenous input provenance in the western Mediterranean.

The role of the eolian input had been partially discussed in the text as we mentioned the papers by Arsouze et al. (2009) and Bout-Roumzeilles et al. (2013). However, following your recommendations, we have added an additional part of the discussion based on the paper by Rodrigo-Gámiz et al. (2015) on the terrigenous input provenance in the western Mediterranean.

In the submitted version of the manuscript, we had cited individual references (Grousset et al., 1992, 1998; Grousset and Biscaye, 2005) that are included in the synthesis paper by Scheuven et al. (2013). In the revised version, we have decided to remove those references and only cite “see synthesis in Scheuven et al., 2013” to make it clear.

Also regarding the Nile discharge, some other recent papers could be considered as Hennekam et al (2014).

This reference has been added to the text of the revised version.

In general, the results on SST are not sufficiently compared with other SST records, see for instance the previously mentioned paper from Martrat et al (2014) and also some recent papers on sea surface temperature variations in the western Mediterranean sea over the last 20 kyr (Rodrigo-Gamiz et al., 2014).

The SU92-33 SST record is now compared to SST reconstructions reported in Martrat et al. (2014) and Rodrigo-Gámiz et al. (2014).

It is also concluded that 18O and 13C values indicate a stratification of the water masses after 16 cal ka BP, but why the data are supporting this conclusion could be further explained in the conclusions section. The implications of the obtained results for the deposition of the ORL1 could also be included in this section.

The deposition of the ORL1 being not the aim of this paper, we do not conclude on potential implications about it.

Reply to reviewer #2 comments:

Thank you very much for agreeing to review this paper and for your comments that have improved the quality of the manuscript.

Most of your comments have been taken into account in the revised version of the manuscript.

Please find below a point-by-point reply relative to your comments.

Introduction. The Introduction could and should be improved and sharpened up (and the same may apply to the discussion). For example (Lines 57-65), the authors seem to build their rationale on the (potential) influence of the Mediterranean thermohaline circulation on the AMOC. But this is not the only reason for better characterising the patterns or variability and the drivers of the thermohaline circulation in this basin. The authors could also (or first) more clearly illustrate the importance of the Mediterranean circulation (an notably of the Levantine Intermediate Waters) for the deep-sea ventilation during the formation of organic-rich deposits (sapropels) across the basin (e.g., De Lange et al., 2008 – Nature Geoscience; Rohling et al., 2015 – Earth-Science Reviews and many others) and/or the more recent evidence of a link between Mediterranean circulation changes and positive phases of the North Atlantic Oscillation (e.g., Incarbona et al., 2016 – Scientific Reports). This would make the introduction section better suited for Climate of the Past by making a more convincing case for the wide relevance of studies like the one by Dubois-Dauphin et al. to the palaeoceanography of the Mediterranean Sea and more generally to our community.

The introduction has been modified by integrating the importance of intermediate and deep water circulation during the formations of organic rich deposits. However, the evidence of a link between Mediterranean circulation changes and positive phases of the North Atlantic Oscillation has not been added as it is relevant only on a decadal timescale, which is not the target of our paper.

Sea Surface Temperature record. The uncertainties associated with the sea surface temperature (SST) reconstructions presented in the paper (Lines 247-255) should be quantitatively assessed. The authors state ‘: : Reliability of SST reconstructions is estimated using a square chord distance test (dissimilarity coefficient), which represents the mean degree of similarity between the sample and the best 10 modern analogues. When the dissimilarity coefficient is lower than 0.25, the reconstruction is considered to be of good quality: : :’. This is a merely qualitative statement; the associated with the SST record presented in the manuscript should instead be quantified.

The uncertainties associated with SST reconstruction have been plotted on figures 2 and 3. Additional information has also been added in the Material and methods section in order to better quantify the SST reconstruction.

Data analysis. I think data generated by Dubois-Dauphin et al. are of high quality, but I also think that their analysis and presentation could and should be improved. For example, could the records in Figure 3b be stacked? This would highlight the main trends in the data and help the reader to easily follow the interpretation presented by the authors (at the moment also because of a ‘wordy’ and fairly unfocused discussion this is not the case). Even better, a Monte Carlo analysis of the data in which both uncertainties in the neodymium isotopes and in the chronology are considered would considerably strengthen the data analysis, allow

more quantitative arguments, and make this a key example for the use of neodymium isotopes to address palaeocirculation problems.

Although both sites in the Balearic and Alboran Sea are likely bathed by the same water mass (LIW), ϵNd records are based on different archives (i.e. cold-water corals and planktonic foraminifera). Furthermore, the age model is different as core SU92-33 is based on ^{14}C measurements while CWC are dated by the U-Th method.

On the other hand, data obtained from CWC from the Sardinia Channel display only specific time slices instead of a continuous record over time.

For these reasons, we do not think that a Monte Carlo analysis and/or a stacked record would be relevant for this study.

Data interpretation. I wonder if the data presented can be so unequivocally interpreted as a reduction of Levantine Intermediate Water (formation? circulation?) during the deposition of sapropel S1 to the extent of arguing for a circulation reversal (which most quantitative analyses so far suggest to be highly unlikely). A possibility that the data cannot rule out is that the Levantine Intermediate Water shoaled rather than weakened and the core sites were bathed by a water mass with a different isotopic fingerprint (e.g., the western Mediterranean intermediate waters proposed by the authors) because of this shoaling.

This alternative hypothesis is now presented at the end of the discussion.

Minor Points

Lines 36-39: text is not very clear; I would recommend rewriting this bit.

The sentence has been slightly rephrased.

Lines 272-283: I think this section can be moved to the methods and merged with sections 3.3.

This section has been re-organised following also recommendations of the reviewer #1

Lines 483-484: What do the authors mean by 'intensity changes'?

We mean changes in LIW production (enhanced or reduced). The sentence has been slightly modified to make it clear.

Hydrological variations of the intermediate water masses of the western Mediterranean Sea during the past 20 ka inferred from neodymium isotopic composition in foraminifera and cold-water corals

Quentin Dubois-Dauphin¹, Paolo Montagna^{2,3}, Giuseppe Siani¹, Eric Douville⁴, Claudia Wienberg⁵, Dierk Hebbeln⁵, Zhifei Liu⁶, Nejjib Kallel⁷, Arnaud Dapoigny⁴, Marie Revel⁸, Edwige Pons-Branchu⁴, [Marco Taviani^{2,9}](#), Christophe Colin^{1*}

Mis en forme : Exposant

¹Laboratoire Geosciences Paris-Sud (GEOPS), Université de Paris Sud, Université Paris-Saclay, 91405 Orsay, France.

²ISMAR-CNR, via Gobetti 101, 40129 Bologna, Italy.

³Lamont-Doherty Earth Observatory, Columbia University, 61 Route 9W, Palisades, NY 10964, USA

⁴Laboratoire des Sciences du Climat et de l'Environnement, LSCE/IPSL, CEA-CNRS-UVSQ, Université Paris-Saclay, F-91191 Gif-sur-Yvette, France.

⁵MARUM-Center for Marine Environmental Sciences, University of Bremen, Leobener Strasse, 28359 Bremen, Germany.

⁶State Key Laboratory of Marine Geology, Tongji University, Shanghai 200092, China.

⁷Laboratoire Georessources, Matériaux, Environnements et Changements Globaux, LR13ES23, Faculté des Sciences de Sfax, Université de Sfax, BP1171, 3000 Sfax, Tunisia.

⁸Geoazur, UNS, IRD, OCA, CNRS, 250 rue Albert Einstein, 06500 Valbonne, ~~France~~France

⁹[Biology Department, Woods Hole Oceanographic Institution, 266 Woods Hole Road, Woods Hole, MA 02543, USA.](#)

Mis en forme : Anglais (États Unis), Exposant

Correspondence to: Christophe Colin (christophe.colin@u-psud.fr)

Abstract. ~~We present~~ ~~the~~ neodymium isotopic composition (ϵNd) of mixed planktonic foraminifera species, ~~from a sediment core collected at 622 m water depth in the Balearic Sea, and as well as~~ ϵNd of scleractinian cold-water corals (CWC; *Madrepora oculata*, *Lophelia pertusa*) ~~collected~~ ~~retrieved~~ at 280-620-414 m water depth in ~~the~~ Balearic Sea, the Alboran Sea and south Sardinian continental margin. ~~The aim was to investigate to~~ constrain hydrological variations at intermediate depths in the western Mediterranean Sea during the last 20 kya. Planktonic (*Globigerina bulloides*) and benthic (*Cibicides pachyderma*) foraminifera were also analyzed for stable oxygen ($\delta^{18}\text{O}$) and carbon ($\delta^{13}\text{C}$) isotopes. The foraminiferal and coral ϵNd values from the Balearic ~~Sea~~ and ~~the~~ Alboran Sea are comparable over the ~~past last~~ ~13 kya, with mean values of -8.94 ± 0.26 (1σ ; $n=24$) and -8.91 ± 0.18 (1σ ; $n=25$), respectively. Before 13 ka BP, the foraminiferal ϵNd values are slightly lower (-9.28 ± 0.15) and tend to reflect a higher mixing between intermediate and deep waters, ~~which is~~ characterized by more unradiogenic ϵNd values. The slight ϵNd increase after 13 ka BP is associated to a ~~marked difference~~ decoupling in the benthic foraminiferal $\delta^{13}\text{C}$ composition ~~of between~~ intermediate and deeper depths, which started at ~16 ka BP. This suggests an earlier stratification of the water masses and a subsequent reduced contribution of unradiogenic ϵNd from deep waters. The CWC from the Sardinia Channel show a much larger scattering of ϵNd values, from -8.66 ± 0.30 to -5.99 ± 0.50 , and a lower average (-7.31 ± 0.73 ; $n=19$) compared to the CWC and foraminifera from the Alboran ~~Sea~~ and Balearic Sea, indicative of intermediate waters sourced from the Levantine basin. At the time of sapropel S1 deposition (10.2 to 6.4 ka), the ϵNd values of the Sardinian CWC become more unradiogenic (-8.38 ± 0.47 ; $n=3$ at ~8.7 ka BP), suggesting a significant contribution of

47 intermediate waters originated from the western basin. Accordingly, we propose ~~here~~ that western Mediterranean
48 intermediate waters replaced the Levantine Intermediate Water (LIW), ~~which was strongly reduced~~ during the
49 mid-sapropel (~8.7 ka BP). This observation supports a notable change of Mediterranean circulation pattern
50 centered on sapropel S1 that needs further investigations to be confirmed.

51

52 1. Introduction

53 The Mediterranean Sea is a mid-latitude semi-enclosed basin, characterized by evaporation exceeding
54 precipitation and river runoff, where the inflow of fresh and relatively warm surface Atlantic water is
55 transformed into saltier and cooler (i.e. denser) intermediate and deep waters. Several studies have demonstrated
56 that the Mediterranean thermohaline circulation was highly sensitive to both the rapid climatic changes
57 propagated into the basin from high latitudes of the Northern Hemisphere (Cacho et al., 1999, 2000, 2002;
58 Moreno et al., 2002, 2005; Paterne et al., 1999; Martrat et al., 2004; Sierro et al., 2005; Frigola et al., 2007,
59 2008) and orbitally-forced modifications of the eastern Mediterranean freshwater budget mainly driven by
60 monsoonal river runoff from the ~~south~~ (Rohling et al., 2002; 2004; Bahr et al., 2015). A link between the
61 intensification of the Mediterranean Outflow Water (MOW) and the intensity of the Atlantic Meridional
62 Overturning Circulation (AMOC) was proposed (Cacho et al., 1999, 2000, 2001; Bigg and Wadley, 2001; Sierro
63 et al., 2005; Voelker et al., 2006) and recently supported by new geochemical data in sediments of the Gulf of
64 Cádiz (Bahr et al., 2015). In particular, it has been suggested that the intensity of the MOW and, more generally,
65 the variations of the thermohaline circulation of the Mediterranean Sea could play a significant role in triggering
66 a switch from a weakened to an enhanced state of the AMOC through the injection of saline Mediterranean
67 waters in the intermediate North Atlantic at times of weak AMOC (Rogerson et al., 2006; Voelker et al., 2006;
68 Khélifi et al., 2009). ~~Since~~ ~~the~~ Mediterranean intermediate waters, notably the Levantine Intermediate Water
69 (LIW), ~~which~~ represent today up to 80 % in volume of the MOW (Kinder and Parilla, 1987) ~~and~~ ~~are~~ ~~therefore~~
70 ~~considered an important key~~ driver of MOW-derived salt into the North Atlantic. ~~Furthermore, it is crucial to~~
71 ~~gain a more complete understanding of the variability of the Mediterranean intermediate circulation in the past~~
72 ~~and its impact on the outflow. the LIW also plays a key role in controlling the deep-sea ventilation of the~~
73 ~~Mediterranean basin, being strongly involved in the formation of deep waters in the Aegean Sea, Adriatic Sea,~~
74 ~~Tyrrhenian Sea and Gulf of Lions (Millot and Taupier-Letage, 2005). It is hypothesized that a reduction of~~
75 ~~intermediate and deep-water formation as a consequence of surface hydrological changes in the eastern~~
76 ~~Mediterranean basin acted as a precondition for the sapropel S1 deposition by limiting the oxygen supply to the~~
77 ~~bottom waters (De Lange et al., 2008; Rohling et al., 2015; Tachikawa et al., 2015). Therefore, it is crucial to~~
78 ~~gain a more complete understanding of the variability of the Mediterranean intermediate circulation in the past~~
79 ~~and its impact on the MOW outflow and, in general, on the Mediterranean thermohaline circulation.~~

80 Previous studies have mainly focused on the glacial variability of the deep-water circulation in the western
81 Mediterranean basin (Cacho et al., 2000, 2006; Sierro et al., 2005; Frigola et al., 2007, 2008). During the Last
82 Glacial Maximum (LGM), strong deep-water convection took place in the Gulf of Lions, producing cold, well-
83 ventilated western Mediterranean Deep Water (WMDW) (Cacho et al., 2000, 2006; Sierro et al., 2005), while
84 the MOW flowed at greater depth in the Gulf of Cádiz (Rogerson et al., 2005; Schönfeld and Zahn, 2000). With
85 the onset of the Termination 1 (T1) at about 15 ka, the WMDW production declined until the ~~transition to the~~
86 Holocene due to the rising sea level, with a relatively weak mode during the Heinrich Stadial 1 (HS1) and the

87 Younger Dryas (YD) (Sierro et al., 2005; Frigola et al., 2008), that led to the deposition of the Organic Rich
88 Layer 1 (ORL1; 14.5-8.2 ka BP; Cacho et al., 2002).

89 Because of the disappearance during the Early Holocene of specific epibenthic foraminiferal species, such as
90 *Cibicidoides* spp., which are commonly used for paleohydrological reconstructions, information about the
91 Holocene variability of the deep-water circulation in the western Mediterranean are relatively scarce and are
92 mainly based on grain size analysis and sediment geochemistry (e.g. Frigola et al., 2007). These authors have
93 identified four distinct phases representing different deep-water overturning conditions in the western
94 Mediterranean basin during the Holocene, as well as centennial- to millennial-scale abrupt events of overturning
95 reinforcement.

96 Faunal and stable isotope records from benthic foraminifera located at intermediate depths in the eastern basin
97 reveal ~~uninterrupted~~ well-ventilated LIW during the last glacial period and deglaciation (Kuhnt et al., 2008;
98 Schmiedl et al., 2010). ~~Similarly, Aa~~ grain-size record obtained from a sediment core collected within the LIW
99 depth range (~500 m water depth) at the east Corsica margin also ~~reveals documents~~ enhanced bottom currents
100 during ~~the glacial period and for specific time intervals during the deglaciation, such as~~ HS1 and ~~the~~ YD
101 (Toucanne et al., 2012). The Early Holocene is characterized by a collapse of the LIW (Kuhnt et al., 2008;
102 Schmiedl et al., 2010; Toucanne et al., 2012) synchronous with the sapropel S1 deposition (10.2 – 6.4 cal ka BP;
103 Mercone et al., 2000). Proxies for deep-water conditions reveal the occurrence of episodes of deep-water
104 overturning reinforcement in the eastern Mediterranean basin at 8.2 ka BP (Rohling et al., 1997, 2015; Kuhnt et
105 al., 2007; Abu-Zied et al., 2008, Siani et al., 2013; Tachikawa et al; 2015), responsible for the interruption of the
106 sapropel S1 in the eastern Mediterranean basin (Mercone et al., 2001; Rohling et al., 2015).

107 Additional insights into Mediterranean circulation changes may be obtained using radiogenic isotopes, such as
108 neodymium, that represent reliable tracers for constraining water-mass mixing and sources (Goldstein and
109 Hemming, 2003, and references therein).

110 It has recently been shown that the neodymium (Nd) isotopic composition, expressed as $\epsilon\text{Nd} =$
111 $(\left[\frac{{}^{143}\text{Nd}}{{}^{144}\text{Nd}} \right]_{\text{sample}} / \left[\frac{{}^{143}\text{Nd}}{{}^{144}\text{Nd}} \right]_{\text{CHUR}} - 1) \times 10000$ (CHUR: Chondritic Uniform Reservoir [Jacobsen and
112 Wasserburg, 1980]) of living and fossil scleractinian CWC faithfully traces intermediate and deep-water mass
113 provenance and mixing of the ocean (e.g. van de Flierdt et al., 2010; Colin et al., 2010; López Correa et al.,
114 2012; Monterro-Serrano et al., 2011, 2013; Copard et al., 2012). Differently from the CWC, the ϵNd
115 composition of fossil planktonic foraminifera is not related to the ambient seawater at calcification depths but
116 reflects the bottom and/or pore water ϵNd , due to the presence of authigenic Fe-Mn coatings precipitated on their
117 carbonate shell (Roberts et al., 2010; Elmore et al., 2011; Piotrowski et al., 2012; Tachikawa et al., 2014; Wu et
118 al., 2015). Therefore, the ϵNd composition of planktonic foraminiferal tests can be used as a useful tracer of
119 deep-water circulation changes in the past, although the effect of pore water on foraminiferal ϵNd values could
120 potentially complicate the interpretation (Tachikawa et al., 2014).

121 In the Mediterranean Sea, modern seawater ϵNd values display a large range from ~-11 to ~-5, and a clear
122 vertical and longitudinal gradient, with more radiogenic values encountered in the eastern basin and typically at
123 intermediate and deeper depths (Spivack and Wasserburg 1988; Henry et al., 1994; Tachikawa et al., 2004;
124 Vance et al., 2004). Considering this large ϵNd contrast, ϵNd recorded in fossil CWC and planktonic
125 foraminifera from the Mediterranean offers great potential to trace intermediate and deep-water mass exchange

126 between the two basins, especially during periods devoid of key epibenthic foraminifera, such as the sapropel S1
127 ~~and/or~~ ORL1 events.

128 Here, the ϵNd of planktonic foraminifera from a sediment core collected in the Balearic Sea and CWC samples
129 from the Alboran Sea and the Sardinia Channel was investigated to establish past changes of the ~~seawater ϵNd~~
130 ~~values~~ at intermediate depths and constrain hydrological variations of the LIW during the ~~past-last~~ ~20 ~~kyra~~. The
131 ϵNd values have been combined with stable oxygen ($\delta^{18}\text{O}$) and carbon ($\delta^{13}\text{C}$) isotope measurements of benthic
132 (*Cibicidoides pachyderma*) and planktonic (*Globigerina bulloides*) foraminifera and sea-surface temperature
133 estimates by modern analogue technique (MAT). Results reveal significant ~~ϵNd changes-~~variations of the E-W~~~~
134 ~~gradient of ϵNd values for the LIW of at intermediate depths in~~ the western basin interpreted ~~by-as~~ a drastic
135 reduction of the hydrological exchanges between the western and eastern Mediterranean Sea and the subsequent
136 higher proportion of intermediate water produced in the Gulf of Lions during the time interval corresponding to
137 the sapropel S1 deposition.

138

139

140

141 2. Seawater ϵNd distribution in the Mediterranean Sea

142 The Atlantic Water (AW) enters the Mediterranean Sea as surface inflow through the Strait of Gibraltar with an
143 unradiogenic ϵNd signature of ~ -9.7 in the strait (Tachikawa et al., 2004) and ~ -10.4 in the Alboran Sea
144 (Tachikawa et al., 2004, Spivack and Wasserburg, 1988) for depths shallower than 50 m. During its eastward
145 flowing, AW mixes with upwelled Mediterranean Intermediate Water forming the Modified Atlantic Water
146 (MAW) that spreads within the basin (Millot and Taupier-Letage, 2005) (Fig.1). The surface water ϵNd values
147 (shallower than 50 m) range from -9.8 to -8.8 in the western Mediterranean basin (Henry et al., 1994; Montagna
148 et al., in prep) and -9.3 to -4.2 in the eastern basin, with seawater off the Nile delta showing the most radiogenic
149 values (Tachikawa et al., 2004; Vance et al., 2004; Montagna et al., in prep). The surface waters in the eastern
150 Mediterranean basin become denser due to strong mixing and evaporation caused by cold and dry air masses
151 flowing over the Cyprus-Rhodes area in winter, and eventually sink leading to the formation of LIW
152 (Ovchinnikov, 1984; Lascaratos et al., 1993, 1998; Malanotte-Rizzoli et al., 1999; Pinardi and Masetti, 2000).
153 The LIW spreads throughout the entire Mediterranean basin at depths between ~ 150 -200 m and ~ 600 -700 m,
154 and is characterized by more radiogenic ϵNd values ranging from -7.9 to -4.8 (average value $\pm 1\sigma$: -6.6 ± 1) in
155 the eastern basin and from -10.4 to -7.58 (-8.7 ± 0.9) in the western basin (Henry et al., 1994; Tachikawa et al.,
156 2004; Vance et al., 2004; Montagna et al., in prep). The LIW acquires its ϵNd signature mainly from the partial
157 dissolution of Nile River particles (Tachikawa et al., 2004), which have an average isotopic composition of -3.25
158 (Weldeab et al., 2002), and the mixing along its path with overlying and underlying water masses with different
159 ϵNd signatures. The LIW finally enters the Atlantic Ocean at intermediate depths through the Strait of Gibraltar
160 with an average ϵNd value of -9.2 ± 0.2 (Tachikawa et al., 2004; Montagna et al., in prep).

161 The WMDW is formed in the Gulf of Lions due to winter cooling and evaporation followed by mixing between
162 ~~the relative fresh~~ surface water and the saline LIW and spreads into the Balearic basin and Tyrrhenian Sea
163 between ~ 2000 m and 3000 m (Millot, 1999; Schroeder et al., 2013) (Fig. 1). The WMDW is characterized by an
164 average ϵNd value of -9.4 ± 0.9 (Henry et al., 1994; Tachikawa et al., 2004; Montagna et al., in prep). Between
165 the WMDW and the LIW (from ~ 700 to 2000 m), the Tyrrhenian Deep Water (TDW) has been found (Millot et

166 al., 2006), which is produced by the mixing between WMDW and Eastern Mediterranean Deep Water (EMDW)
167 that cascades in the Tyrrhenian Sea after entering ~~from~~ the Strait of Sicily (Millot, 1999, 2009; Astraldi et al.,
168 2001). The TDW has an average ϵNd value of -8.1 ± 0.5 (Montagna et al., in prep).

169

170

3. Material and methods

171

3.1. Cold-water coral and foraminifera samples

172

Forty-four CWC samples belonging to the species *Lophelia pertusa* and *Madrepora oculata* collected from the
173 Alboran Sea and the Sardinia Channel were selected for this study (Fig. 1). Nineteen fragments were collected at
174 various core depths from a coral-bearing sediment core (RECORD 23; 38°42.18' N; 08°54.75' E; Fig. 1)
175 retrieved from 414 m water depth in the "Sardinian Cold-Water Coral Province" (Taviani et al., 2015) during the

176

R/V Urania cruise "RECORD" in 2013. The core contains well-preserved fragments of *M. oculata* and *L.*
177 *pertusa* embedded in a brownish muddy to silty carbonate-rich sediment. The Sardinian CWC samples were

Mis en forme : Police :Italique

177

Mis en forme : Police :Italique

178

used for U-series dating and Nd isotopic composition measurements. For the southern Alboran Sea, twenty-five
179 CWC samples were collected at water depths between 280 and 442 m in the "eastern Melilla Coral Province"
180 (Fig. 1) during the R/V Poseidon cruise "POS-385" in 2009 (Hebbeln et al., 2009). Eleven samples were
181 collected at the surface of two coral mounds (New Mound and Horse Mound) and three coral ridges (Brittlestar
182 ridges I, II and III), using a box corer and a remotely operated vehicle (ROV). In addition, fourteen CWC
183 samples were collected from various core depths of three coral-bearing sediment cores (GeoB13728, 13729 and
184 13730) retrieved from the Brittlestar ridge I. Details on the location of surface samples and cores collected in the
185 southern Alboran Sea and details on the radiocarbon ages obtained from these coral samples are reported in Fink
186 et al. (2013). Like the CWC sample set from the Sardinia Channel, the dated Alboran CWC samples were also
187 used for further Nd isotopic composition analyses in this study.

188

In addition, a deep-sea sediment core (barren of any CWC fragments) was recovered in the southwest of the
189 Balearic Sea at 622 m water depth during the R/V Le Suroît cruise "PALEOCINAT II" in 1992 (SU92-33;
190 35°25.38' N; 0°33.86' E; Fig. 1). The core unit, which consists of 2.1 m of grey to brown carbonaceous clays,
191 and was sub-sampled continuously at 5-10 cm intervals for the upper 2.1 m for a total number of 24 samples
192 used for $\delta^{18}\text{O}$, $\delta^{13}\text{C}$ and ϵNd further multi-proxy analyzes.

193

194

3.2. Analytical procedures on cold-water coral samples

195

3.2.1. U/Th dating

196

The nineteen CWC samples collected from the sediment core RECORD 23 (Sardinia Channel) were analysed for
197 uranium and thorium isotopes to obtain absolute dating using a Thermo Scientific™ Neptune^{Plus} MC-ICPMS
198 installed at the Laboratoire des Sciences du Climat et de l'Environnement (LSCE, Gif-sur-Yvette, France). Prior
199 to analysis, the samples were carefully cleaned using a small diamond blade to remove any visible contamination
200 and sediment-filled cavities. The fragments were examined under a binocular microscope to ensure against the
201 presence of bioeroded zones and finally crushed into a coarse-grained powder with an agate mortar and pestle.
202 The powders (~60-100 mg) were transferred to acid cleaned Teflon beakers, ultrasonicated in MilliQ water,
203 leached with 0.1N HCl for ~ 15 s and finally rinsed twice with MilliQ water. The physically and chemically
204 cleaned samples were dissolved in 3-4 ml dilute HCl (~10%) and mixed with an internal triple spike with known
205 concentrations of ^{229}Th , ^{233}U and ^{236}U , calibrated against a Harwell Uraninite solution (HU-1) assumed to be at

206 secular equilibrium. The solutions were evaporated to dryness at 70°C, redissolved in 0.6 ml 3N HNO₃ and then
207 loaded into 500 µl columns packed with Eichrom UTEVA resin to isolate uranium and thorium from the other
208 major and trace elements of the carbonate matrix. The U and Th separation and purification followed a
209 procedure slightly modified from Douville et al. (2010). The U and Th isotopes were determined following the
210 protocol recently revisited at LSCE (Pons-Branchu et al., 2014). The ²³⁰Th/U ages were calculated from
211 measured atomic ratios through iterative age estimation (Ludwig and Titterton, 1994), using the ²³⁰Th, ²³⁴U
212 and ²³⁸U decay constants of Cheng et al. (2013) and Jaffey et al. (1971). Due to the low ²³²Th concentration (< 1
213 ng/g; see Table 1), no correction was applied for the non-radiogenic ²³⁰Th fraction.

214

215 3.2.2 Nd isotopic composition analyses on cold-water coral fragments


216 Sub-samples of the CWC fragments from the Sardinia Channel used for U-series dating in this study (Table 1) as
217 well as sub-samples of the twenty-five CWC fragments originating from the Alboran Sea, which were already
218 radiocarbon-dated by Fink et al. (2013) (Table 2), were used for further Nd isotopic composition analyses. The
219 fragments (350 to 600 mg) were subjected to a mechanical and chemical cleaning procedure. The visible
220 contaminations, such as Fe-Mn coatings and detrital particles, were carefully removed from the inner and
221 outermost surfaces of the coral skeletons using a small diamond blade. The physically cleaned fragments were
222 ultrasonicated for 10 min with 0.1 N ultra-clean HCl, followed by several MilliQ water rinses and finally
223 dissolved in 2.5 N ultraclean HNO₃. Nd was separated from the carbonate matrix using Eichrom TRU and LN
224 resins, following the analytical procedure described in detail in Copard et al. (2010).

225 The ¹⁴³Nd/¹⁴⁴Nd ratios of all purified Nd fractions were analyzed using the ThermoScientific Neptune^{Plus} Multi-
226 Collector Inductively Coupled Plasma Mass Spectrometer (MC-ICP-MS) hosted at LSCE. The mass-
227 fractionation correction was made by normalizing ¹⁴⁶Nd/¹⁴⁴Nd to 0.7219 and applying an exponential law.
228 During each analytical session, samples were systematically bracketed with analyses of JNdi-1 and La Jolla
229 standard solutions, which are characterised by accepted values of 0.512115±0.000006 (Tanaka et al., 2000) and
230 0.511855±0.000007 (Lugmair et al., 1983), respectively. Standard JNdi-1 and La Jolla solutions were analysed
231 at concentrations similar to those of the samples (5-10 ppb) and all the measurements affected by instrumental
232 bias were corrected, when necessary, using La Jolla standard. The external reproducibility (2σ) for time resolved
233 measurement, deduced from repeated analyses of La Jolla and JNdi-1 standards, ranged from 0.1 to 0.5 εNd
234 units for the different analytical sessions. The analytical error for each sample analysis was taken as the external
235 reproducibility of the La Jolla standard for each session. Concentrations of Nd blanks were negligible compared
236 to the amount of Nd of CWC investigated in this study.

237

238 3.3. Analyses on sediment of core SU92-33

239 3.3.1. Radiocarbon dating

240 Radiocarbon dating was measured at UMS-ARTEMIS (Pelletron 3MV) AMS (CNRS-CEA Saclay, France).
241 Seven AMS radiocarbon (¹⁴C) dating were performed in core SU92-33 on well-preserved calcareous tests of the
242 planktonic foraminifera *G. bulloides* in the size fraction >150 µm (Table 3). The age model for the core was
243 derived from the calibrated planktonic ages by applying a mean reservoir effect of ~400 years (Siani et al., 2000,
244 2001). All ¹⁴C ages were converted to calendar years (cal. yr BP, BP = AD 1950) by using the INTCAL13
245 calibration data set (Reimer et al., 2013) and the CALIB 7.0 program (Stuiver and Reimer, 1993). 

246

247

3.3.2. Stable isotopes

248

249

250

251

252

253

254

Stable oxygen ($\delta^{18}\text{O}$) and carbon ($\delta^{13}\text{C}$) isotope measurements were performed in core SU92-33 on well-preserved (clean and intact) samples of the planktonic foraminifera *G. bulloides* (250-315 μm fraction) and the epibenthic foraminifera *C. pachyderma* (250-315 μm fraction) using a Finnigan MAT-253 mass spectrometer at the State Key Laboratory of Marine Geology (Tongji University). Both $\delta^{18}\text{O}$ and $\delta^{13}\text{C}$ values are presented relative to the Pee Dee Belemnite (PDB) scale by comparison with the National Bureau of Standards (NBS) 18 and 19. The mean external reproducibility was checked by replicate analyses of laboratory standards and is better than $\pm 0.07\text{‰}$ (1σ) for $\delta^{18}\text{O}$ and $\pm 0.04\text{‰}$ for $\delta^{13}\text{C}$.

255

3.3.3 Nd isotope measurements on planktonic foraminifera

256

257

258

259

260

261

262

263

264

Approximately 25 mg of mixed planktonic foraminifera species were picked from the $>63\ \mu\text{m}$ size fraction of each sample already used for stable isotope measurements (Table 4). The samples were gently crushed between glass slides under the microscope to ensure that all chambers were open, and ultrasonicated with MilliQ water. Samples were allowed to settle between ultrasonication steps before removing the supernatant. Each sample was rinsed thoroughly with MilliQ water until the solution was clear and free of clay. The cleaned samples were dissolved in 1N acetic acid and finally centrifuged to ensure that all residual particles were removed, following the procedure described in Roberts et al. (2010). Nd was separated following the analytical procedure reported in Wu et al. (2015). For details on the measurement of Nd isotopes see the section above.

265

3.3.4. Modern analogue technique (MAT)

266

267

268

269

270

271

272

273

274

275

276

277

The palaeo-sea surface temperatures (SST) were estimated using the modern analogue technique (MAT) (Hutson, 1980; Prell, 1985), implemented by Kallel et al. (1997) for the Mediterranean Sea. This method directly measures the difference between the faunal composition of a fossil sample with a modern database, and it identifies the best modern analogues for each fossil assemblage (Prell, 1985). Reliability of SST reconstructions is estimated using a square chord distance test (dissimilarity coefficient), which represents the mean degree of similarity between the sample and the best 10 modern analogues. When the dissimilarity coefficient is lower than 0.25, the reconstruction is considered to be of good quality (Overpeck et al., 1985; Kallel et al., 1997). For core SU92-33, good similarity coefficients are <0.2 , with an average value of ~ 0.13 (varying between 0.07 and 0.19; Fig. 2a). The calculated mean standard deviation of SST estimates observed in core MD90-917 are $\sim 1.5\ ^\circ\text{C}$ from the late glacial period to the Younger Dryas and $\sim 1.2\ ^\circ\text{C}$ during for the Holocene and $\sim 1.5\ ^\circ\text{C}$ since the late glacial period until the Younger Dryas.

278

4. Results

279

4.1. Cold-water corals ages

280

281

282

283

284

285

The good state of preservation for the CWC samples from the Sardinia Channel (RECORD 23; Fig. 1) is attested by their initial $\delta^{234}\text{U}$ values (Table 1), which is in the range of the modern seawater value (146.8 ± 0.1 ; Andersen et al., 2010). If the uncertainty of the $\delta^{234}\text{U}$ is taken into account, all the values fulfill the so-called “strict” $\pm 4\ \text{‰}$ reliability criterion and the U/Th ages can be considered strictly reliable. The coral ages range from 0.091 ± 0.011 to 10.904 ± 0.042 ka BP (Table 1), and reveal three distinct clusters of coral age distribution during the Holocene representing periods of sustained coral occurrence. These periods coincide with the Early Holocene

286 encompassing a 700-years-lasting time interval from ~10.9 to 10.2 ka BP, the very late Early Holocene at ~8.7
287 ka BP, and the Late Holocene starting at ~1.5 ka BP (Table 1).

288 Radiocarbon ages obtained for CWC samples collected in the Alboran Sea were published by Fink et al. (2013)
289 (Table 2). They also document three periods of sustained CWC occurrence coinciding with the Bølling–Allerød
290 (B-A) interstadial (13.5–12.9 cal ka BP), the Early Holocene (11.2–9.8 cal ka BP) and the Mid- to Late Holocene
291 (5.4–0.3 cal ka BP).

292 The ϵ Nd record obtained from the CWC samples from the Alboran Sea displays a narrow range from -
293 9.22±0.30 to -8.59±0.3, which is comparable to the ϵ Nd record obtained on of the planktonic foraminifera from
294 the Balearic Sea over the last 13.5 kyr (Table 2, Fig. 3b). Most of the CWC ϵ Nd values are similar within error
295 and the record does not reveal any clear difference over the last ~13.5 kyr.

296 On the contrary, Finally, the CWC samples from the Sardinia Channel display a relatively large ϵ Nd range, with
297 values values ranging varying from -5.99±0.50 to -7.75±0.10 during the Early and Late Holocene, and values as
298 low as -8.66±0.30 during the the mid-sapropel S1 deposition (S1a) at (~8.7 ka BP) (Table 1, Fig. 3c).

299

300

301 4.2 Chronological framework for core Core SU92-33

302 The stratigraphy of core SU92-33 was derived from the $\delta^{18}\text{O}$ variations of the planktonic foraminifera
303 *G. bulloides* (Fig. 2b). The last glacial/interglacial transition and the Holocene encompasses the upper 2.1 m of
304 the core (Fig. 2b). The $\delta^{18}\text{O}$ record of *G. bulloides* shows higher values (~3.5 ‰) during the late glacial
305 compared to the Holocene (from ~1.5 to 0.8 ‰) exhibiting a pattern similar to those observed in nearby deep-sea
306 cores from the Western Mediterranean Sea (Sierra et al., 2005; Melki et al., 2009).

307 The age model for the upper 1.2 m of the core of core SU92-33 is-was based on 7 AMS- ^{14}C age
308 measurements for the upper 1.2 m of the core and a by a linear interpolation between these ages (Table 3, Fig. 2).
309 For the lower portion of the coreBelow, a control point has-been-was established for-at the onset of the last
310 deglaciation, which is-that presents-a coeval age-in the western and central Mediterranean Sea at ~about 17 cal
311 ka BP (Sierra et al., 2005; Melki et al., 2009; Siani et al., 2001). Overall, The upper 2.1 m of core SU92-33
312 spans the last 19 kyr, with an estimated average sedimentation rate ranging from ~15 cm ka⁻¹ during the
313 deglaciation to ~10 cm ka⁻¹ between 9 to 15 cm ka⁻¹, with the lowest values observed during the Holocene.

314

315 4.3 SST reconstructions of core SU92-33

316 April-May SST reconstruction was derived from MAT to define the main climatic events recorded in
317 core SU92-33 during the last 19 kyr. SSTs vary from 8.5°C to 17.5°C with high amplitude variability over the
318 last 19 kyr BP (Fig. 2a). The LGM (19-18 ka BP) is characterized by SST values centered at around 12°C.
319 Then, a progressive decrease of ~4°C between 17.8 ka and to 16 ka marks the Heinrich Stadial 1 (HS1) (Fig. 2a).
320 A warming phase (~14°C) between 14.5 ka BP and 13.8 ka BP coincides with the B-A interstadial and is
321 followed by a cooling (~11°C) between 13.1 ka BP and 11.8 ka BP largely corresponding to the YD (Fig. 2a).
322 During the Holocene, SSTs show mainly values of ~16°C, with one exception between 7 ka BP and 6 ka BP
323 pointing to an abrupt cooling of ~3°C (Fig. 2a). From the late glacial to the Holocene, SST variations show a
324 similar pattern to that previously observed in the Gulf of Lions and Tyrrhenian Sea (Kallel et al., 1997; Melki et
325 al., 2009) as well as in the Alboran Sea (Martrat et al., 2014; Rodrigo-Gámiz et al., 2014) and. They are globally

326 synchronous for the main climatic transitions to the well dated South Adriatic Sea core MD90-917 (Siani et al.,
327 2004) confirming the robustness of the SU92-33 age model (Fig. 2a).

328 ~~4.4 Benthic stable oxygen and carbon isotope records of core SU92-33~~

329 The $\delta^{18}\text{O}$ and $\delta^{13}\text{C}$ records obtained from the benthic foraminifera *C. pachyderma* display significant variations
330 at millennial time scales (Figs. 2c and 2d). The $\delta^{18}\text{O}$ values decrease steadily from $\sim 4.5\text{‰}$ during the LGM to
331 $\sim 1.5\text{‰}$ during the Holocene, without showing any significant excursion during HS1 and the YD events (Fig.
332 2c), in agreement with results obtained from the neighbor core MD99-2343 (Sierra et al., 2005).

333 The $\delta^{13}\text{C}$ record obtained from *C. pachyderma* shows a decreasing trend since the LGM with a low variability
334 from $\sim 1.6\text{‰}$ to $\sim 0.6\text{‰}$ (Fig. 2d). The heaviest $\delta^{13}\text{C}$ values are related to the LGM ($\sim 1.6\text{‰}$) while the lightest
335 values ($\sim 0.6\text{‰}$) characterize the Early Holocene and in particular the period corresponding to the sapropel S1
336 event in the eastern Mediterranean basin (Fig. 2d).

337 ~~The~~

338 ~~4.5 Nd isotopic composition of planktonic foraminifera and cold water corals~~

339 ϵNd values of planktonic foraminifera of core SU92-33 collected from the Balearic Sea vary within a relatively
340 narrow range between -9.50 ± 0.30 and -8.61 ± 0.30 , with an average value of -9.06 ± 0.28 (Table 2, Fig. 3b). The
341 record shows a slight increasing trend since the LGM, with the more unradiogenic values (average -9.28 ± 0.15 ;
342 $n=7$) being observed in the oldest part of the record (between 18 and 13.5 ka BP), whereas Holocene values are
343 generally more radiogenic (average -8.84 ± 0.22 ; $n=17$) (Fig. 3b).

344 ~~The ϵNd record obtained for the CWC samples from the Alboran Sea displays a narrow range from -9.22 ± 0.30 to~~
345 ~~-8.59 ± 0.3 , which is comparable to the ϵNd record obtained on planktonic foraminifera from the Balearic Sea~~
346 ~~over the last 13.5 ka (Table 2, Fig. 3b). Most of the CWC ϵNd values are similar within error and the record does~~
347 ~~not reveal any clear difference over the last 13.5 ka.~~

348 ~~Finally, the CWC samples from the Sardinia Channel display ϵNd values ranging from -5.99 ± 0.50 to -7.75 ± 0.10~~
349 ~~during the Early and Late Holocene, and values as low as -8.66 ± 0.30 during the the mid sapropel S1 deposition~~
350 ~~(S1a) (~ 8.7 ka BP) (Table 1, Fig. 3c).~~

351 5. Discussion

352 ~~As first observations~~ Overall, the CWC and foraminiferal ϵNd values measured for in this study indicate point to
353 a pronounced dispersion at intermediate depth in terms of absolute values and variability in Nd isotopes during
354 the Holocene between the Alboran and Balearic Seas and the Sardinia Channel. In addition Furthermore, the
355 foraminiferal ϵNd record reveals an evolution towards more radiogenic values at intermediate water depth in the
356 Balearic Sea over the last ~ 19 kyra (Fig. 3).

357 A prerequisite to properly interpret such ϵNd values differences and variations through time consists in
358 characterizing first the present-day ϵNd of the main water-mass end-members circulating-flowing in the western
359 Mediterranean basin. This is possible It is also necessary to by evaluating the temporal changes in ϵNd of the
360 end-members since the LGM, and assessing the potential influences of lithogenic Nd input and regional
361 exchange between the continental margins and seawater ("boundary exchange"; Lacan and Jeandel, 2001, 2005)
362 on the ϵNd values of intermediate water masses.

Mis en forme : Police :Times New Roman

Mis en forme : Police :Times New Roman

Mis en forme : Police :Times New Roman

Mis en forme : Police :Times New Roman

Mis en forme : Police :Times New Roman

Mis en forme : Police :Times New Roman

Mis en forme : Police :Times New Roman

Mis en forme : Police :Times New Roman

365 During its westward flow, the LIW continuously mixes with surrounding waters with different ϵNd signatures
366 lying above and below. For the western Mediterranean basin, these water masses are the MAW/Western
367 Intermediate Water (WIW) and the TDW/WMDW, respectively. Accordingly, a well-defined and gradual ϵNd
368 gradient exists at intermediate depth between the eastern and western Mediterranean basins, with LIW values
369 becoming progressively more unradiogenic towards the Strait of Gibraltar, from -4.8 ± 0.2 at 227 m in the
370 Levantine basin to -10.4 ± 0.2 at 200 m in the Alboran Sea (Tachikawa et al., 2004). Such an ϵNd pattern implies
371 an effective vertical mixing with more unradiogenic water masses along the E-W LIW trajectory ruling out
372 severe isotopic modifications of the LIW due to the local exchange between the continental margins and
373 seawater. Unfortunately, no information exists on the potential temporal variability in ϵNd of the Mediterranean
374 water-mass end-members since the LGM.

375 It has been demonstrated that eolian dust input can modify the surface and sub-surface ϵNd distribution of the
376 ocean in some areas (Arsouze et al., 2009). The last glacial period was associated with an aridification of North
377 Africa (Sarnthein et al., 1981; Hooghiemstra et al., 1987; Moreno et al., 2002; Wienberg et al., 2010) and higher
378 fluxes of Saharan dust to the NE tropical Atlantic (Itambi et al., 2009) and the western Mediterranean Sea
379 characterized by unradiogenic ϵNd values (between -10.1 ± 0.4 and -17.14 ± 0.4 ; ~~Grousset et al., 1992, 1998;~~
380 ~~Grousset and Biscaye, 2005; see synthesis in Scheuven et al., 2013~~). Bout-Roumazeilles et al. (2013)
381 documented a dominant role of eolian supply in the Siculo-Tunisian Strait during the last 20 ka, with the
382 exception of a significant riverine contribution (from the Nile River) and a strong reduction of eolian input
383 during the sapropel S1 event. Such variations in the eolian input to the Mediterranean Sea are not associated to a
384 significant change in the seawater ϵNd record obtained for the Balearic Sea (core SU92-33) during the sapropel
385 S1 event (Fig. 3). Furthermore, the ϵNd signature of the CWC from the Sardinia Channel (core RECORD 23)
386 shifts to more unradiogenic values (-8.66 ± 0.30) during the sapropel S1 event, which is opposite to what expected
387 if it was related to a strong reduction of eolian sediment input. In a recent study, addition, Rodrigo-Gámiz et al.
388 (2015) have documented variations in the terrigenous provenance from a sediment record in the Alboran Sea
389 (core 293G; 36°10.414'N, 2°45.280'W, 1840 m water depth) since the LGM. Radiogenic isotopes (Sr, Nd, Pb)
390 point to changes from North African dominated sources during the glacial period to European dominated source
391 during the Holocene. Nevertheless, the major Sr-Nd-Pb excursions documented by Rodrigo-Gámiz et al. (2015)
392 and dated at ca. 11.5, 10.2, 8.9-8.7, 5.6, 2.2 and 1.1, ka cal BP do not seem to affect the ϵNd values of our
393 foraminifera and coral records.

394 ~~Thus, all~~ Taken together, these results suggest that changes of eolian dust input since the LGM were not
395 responsible for the observed ϵNd variability at intermediate water depths.

396 Consequently, assuming that the Nd isotopic budget of the western Mediterranean Sea has not been strongly
397 modified since the LGM, the reconstructed variations of the E-W gradient of ϵNd values in the western
398 Mediterranean Sea for the past and notably during the sapropel S1 event (Fig. 3) are indicative of a major
399 reorganization of intermediate water circulation.

400

401 *5.1 Hydrological changes in the Alboran and Balearic Seas since the LGM*

402 The range in ϵNd for the CWC from the Alboran Sea (from -9.22 ± 0.30 to -8.859 ± 0.30 ; Table 2) is very close to
403 the one obtained for the planktonic foraminifera from the Balearic Sea (from -9.50 ± 0.30 to -8.61 ± 0.30 ; Table 4,
404 Fig. 3c), suggesting that both sites are influenced by the same intermediate water masses at least for the last 13.5

Mis en forme : Police :10 pt, Anglais
(États Unis)

kyra BP. Today, LIW occupies a depth range between ~200 and ~700 m in the western Mediterranean basin (Millot, 1999; Sparnocchia et al., 1999). More specifically, the salinity maximum corresponding to the core of LIW is found at around 400 m in the Alboran Sea (Millot, 2009) and up to 550 m in the Balearic Sea (López-Jurado et al., 2008). The youngest CWC sample collected in the Alboran Sea with a rather "recent" age of 0.34 cal ka BP (Fink et al. 2013) displays an ϵNd value of -8.59 ± 0.30 (Table 2) that is similar to the present-day value of the LIW at the same site (-8.3 ± 0.2) (Dubois-Dauphin et al., submitted) and is significantly different from the WMDW ϵNd signature in the Alboran Sea (-10.7 ± 0.2 , 1270 m water depth; Tachikawa et al., 2004). Considering the intermediate depth range of the studied CWC and foraminifera samples, we can reasonably assume that samples from both sites, in the Balearic Sea (622 m water depth) and in the Alboran Sea (280 to 442 m water depth), record ϵNd variations of the LIW. The ϵNd record obtained from planktonic foraminifera generally displays more unradiogenic and homogenous values before ~13 cal ka BP (range from -9.46 to -9.12) compared to the most recent part of the record (range from -9.50 to -8.61), with the highest value of -8.61 ± 0.3 in the Early and Late Holocene.

[The SST record displays values centered at around 12°C during the LGM with a subsequent rapid SST decrease towards 9°C, highlighting the onset of the HS1 \(Fig. 2a\). These values are well comparable to recent high-resolution SST data obtained in the Alboran Sea \(Martrat et al., 2014; Rodrigo-Gámiz et al., 2014\).](#)

The $\delta^{18}\text{O}$ record obtained on *G. bulloides* indicates an abrupt 1‰ excursion towards lighter values centered at about 16 cal ka BP (Table 4), synchronous with the HS1 (Fig. 2b), which is similar to the $\delta^{18}\text{O}$ shift reported by Sierro et al. (2005) for a core collected at 2391 m water depth NE of the Balearic Islands (MD99-2343; Fig. 1). As the Heinrich events over the last glacial period are characterized by colder and fresher surface water in the Alboran Sea (Cacho et al., 1999; Pérez-Folgado et al., 2003; Martrat et al., 2004, 2014; Rodrigo-Gámiz et al., 2014) and dry climate on land over the western Mediterranean Sea (Allen et al., 1999; Combourieu-Nebout et al., 2002; Sanchez Goni et al., 2002; Bartov et al., 2003), lighter $\delta^{18}\text{O}$ values of planktonic *G. bulloides* are thought to be the result of the inflow of freshwater derived from the melting of icebergs in the Atlantic Ocean into the Mediterranean Sea (Sierro et al., 2005; Rogerson et al., 2008).

During this time interval, the $\delta^{13}\text{C}$ record of *C. pachyderma* from the Balearic Sea (core SU92-33) displays a decreasing $\delta^{13}\text{C}$ trend after ~16 cal ka BP (from 1.4 ‰ to 0.9 ‰; Table 4; Fig. 4a). Moreover, the $\delta^{13}\text{C}$ record obtained on benthic foraminifera *C. pachyderma* from the deep Balearic Sea (core MD99-2343) reveals similar $\delta^{13}\text{C}$ values before ~16 cal ka BP suggesting well-mixed and ventilated water masses during the LGM and the onset of the deglaciation (Sierro et al., 2005).

The slightly lower foraminiferal ϵNd values before ~13 cal ka BP could reflect a stronger influence of water masses deriving from the Gulf of Lions as WMDW (ϵNd : -9.4 ± 0.9 ; Henry et al., 1994; Tachikawa et al., 2004; Montagna et al., in prep). This is in agreement with ϵNd results obtained by Jiménez-Espejo et al. (2015) from planktonic foraminifera collected from deep-water sites (1989 m and 2382 m) in the Alboran Sea (Fig. 4c). Jiménez-Espejo et al. (2015) documented lower ϵNd values (ranging from -10.14 ± 0.27 to -9.58 ± 0.22) during the LGM, suggesting an intense deep-water formation. This is also associated to an enhanced activity of the deeper branch of the MOW in the Gulf of Cádiz (Rogerson et al., 2005; Voelker et al., 2006) linked to the active production of the WMDW in the Gulf of Lions during the LGM (Jiménez-Espejo et al., 2015).

The end of the HS1 (14.7 cal ka BP) is concurrent with the onset of the B-A warm interval characterized by increased SST [up to 4°C in the Balearic Sea \(SU92-33; Fig. 3a\), also](#) identified for various sites in the

445 Mediterranean Sea (Cacho et al., 1999; Martrat et al., 2004, 2014; Essallami et al., 2007; [Rodrigo-Gámiz et al.,](#)
446 [2014](#)), in agreement with the SST record obtained for the Balearic Sea (SU92-33; Fig. 3a). The B-A interval is
447 associated ~~with~~ the so-called melt-water pulse 1A (e.g. Weaver et al., 2003) occurring at around 14.5 cal ka
448 BP. This led to a rapid sea-level rise of about 20 m in less than 500 years and large freshwater discharges in the
449 Atlantic Ocean due to the melting of continental ice sheets (Deschamps et al., 2012), resulting in an enhanced
450 Atlantic inflow across the Strait of Gibraltar. Synchronously, cosmogenic dating of Alpine glacier retreat
451 throughout the western Mediterranean hinterland suggests maximum retreat rates (Ivy-Ochs et al., 2007; Kelly et
452 al., 2006). Overall, these events are responsible for freshening Mediterranean waters and reduced surface water
453 density, and hence, weakened ventilation of intermediate (Toucanne et al., 2012) and deep-water masses (Cacho
454 et al., 2000; Sierro et al., 2005). Similarly, lower benthic $\delta^{13}\text{C}$ values obtained for the Balearic Sea (Fig. 4a) point
455 to less ventilated intermediate water relative to the late glacial. In addition, a decoupling in the benthic $\delta^{13}\text{C}$
456 values is observed between deep (MD99-2343) and intermediate (core SU92-33) waters after ~16 cal ka BP
457 (Sierro et al. 2005), suggesting an enhanced stratification of the waters masses (Fig. 4a). At this time, the
458 shallowest ϵNd record from the deep Alboran Sea (core 300G) shifted towards more radiogenic values, while the
459 deepest one (core 304G) remained close to the LGM values (Jimenez-Espejo et al., 2015) (Fig. 4c). Furthermore,
460 results from the UP10 fraction (particles > 10 μm) of the MD99-2343 sediment core (Fig. 4d), indicate a
461 declining bottom-current velocity at 15 ka BP (Frigola et al., 2008). Rogerson et al. (2008) have hypothesized
462 that during deglacial periods the sinking depth of dense waters produced in the Gulf of Lions was shallower
463 resulting in new intermediate water (WIW) rather than new deep-water (WMDW) as observed today during mild
464 winters (Millot, 1999; Schott et al., 1996). Therefore, intermediate depths of the Balearic Sea could have been
465 isolated from the deep-water with the onset of the T1 (at ~15 ka BP). The reduced convection in the deep
466 western Mediterranean Sea together with the shoaling of the nutricline (Rogerson et al., 2008) led to the
467 deposition of the ORL 1 (14.5 to 8.2 ka B.P; Cacho et al., 2002) and dysoxic conditions below 2000 m in
468 agreement with the absence of epibenthic foraminifera such as *C. pachyderma* after 11 cal ka BP in MD99-2343
469 (Sierro et al., 2005) (Fig. 4a).

470 After 13.5 ka BP, planktonic foraminifera ϵNd values from the Balearic Sea (core SU92-33) become more
471 radiogenic and are in the range of CWC ϵNd values from the Alboran Sea (Fig. 4b). These values may reveal a
472 stronger influence of the LIW in the Balearic Sea during the Younger Dryas, as also supported by the sortable
473 silt record from the Tyrrhenian Sea (Toucanne et al., 2012) (Fig. 4e). Deeper depths of the Alboran Sea also
474 record a stronger influence of the LIW with an ϵNd value of -9.1 ± 0.4 (Jimenez-Espejo et al., 2015). In addition,
475 a concomitant activation of the upper MOW branch, as reconstructed from higher values of Zr/Al ratio in
476 sediments of the Gulf of Cádiz, can be related to the enhanced LIW flow in the western Mediterranean Sea (Fig.
477 4f) (Bahr et al., 2015).

478 The time of sapropel S1 deposition (10.2 – 6.4 ka) is characterized by a weakening or a shutdown of
479 intermediate- and deep-water formation in the eastern Mediterranean basin (Rossignol-Strick et al., 1982; Cramp
480 and O’Sullivan, 1999; Emeis et al., 2000; Rohling et al., 2015). At this time, planktonic foraminifera ϵNd values
481 from intermediate water depths in the Balearic Sea (core SU92-33) remain high (between -9.15 ± 0.3 and $-$
482 8.61 ± 0.3) (Fig. 4b). On the other hand, the deeper Alboran Sea provides a value of -9.8 ± 0.3 pointing to a
483 stronger contribution of WMDW (Jimenez-Espejo et al., 2015), coeval with the recovery of deep-water activity
484 from core MD99-2343 (Frigola et al., 2008).

485
486

5.2 Hydrological changes in the Sardinia Channel during the Holocene

487 The present-day hydrographic structure of the Sardinia Channel is characterized by four water masses, with the
488 surface, intermediate and deep-water masses being represented by MAW, LIW and TDW/WMDW, respectively
489 (Astraldi et al., 2002a; Millot and Taupier-Lepage, 2005). In addition, the WIW, flowing between the MAW and
490 the LIW, has also been observed along the Channel (Sammari et al., 1999). The core of the LIW is located at
491 400-450 m water depth in the Tyrrhenian Sea (Hopkins, 1988; Astraldi et al., 2002b), which is the depth range of
492 CWC samples from the Sardinia Channel (RECORD 23; 414 m) (Taviani et al., 2015). The youngest CWC
493 sample dated at ~0.1 ka BP has an ϵNd value of -7.70 ± 0.10 (Table 1, Fig. 5), which is similar within error to the
494 value obtained from a seawater sample collected at 451 m close to the coral sampling location (-8.0 ± 0.4 ;
495 Montagna et al., in prep).

496 The CWC dating from the Sardinia Channel shows three distinct periods of sustained coral occurrence in this
497 area during the Holocene, with each displaying a large variability in ϵNd values. CWC from the Early Holocene
498 (10.9-10.2 ka BP) and the Late Holocene (<1.5 ka BP) exhibit similar ranges of ϵNd values (ranging from -
499 5.99 ± 0.50 to -7.75 ± 0.20 ; Table 1, Fig 5c). Such variations are within the present-day ϵNd range being
500 characteristic for intermediate waters in the eastern Mediterranean Sea (-6.6 ± 1.0 ; Tachikawa et al., 2004; Vance
501 et al., 2004). However, the CWC ϵNd values are more radiogenic than those observed at mid-depth in the
502 present-day western basin (ranging from -10.4 ± 0.2 to -7.58 ± 0.47 ; Henry et al., 1994; Tachikawa et al., 2004;
503 Montagna et al., in prep), suggesting a stronger LIW component in the Sardinia Channel during the Early and
504 Late Holocene. The Sardinian CWC ϵNd variability also reflects the sensitivity of the LIW to changes in the
505 eastern basin such as rapid variability of the Nile River flood discharge (Revel et al., 2014; 2015; Weldeab et al.,
506 2014) or a modification through time in the proportion between the LIW and the Cretan Intermediate Water
507 (CIW). Today, the intermediate water outflowing from the Strait of Sicily is composed by ~66 to 75 % of LIW
508 and 33 to 25 % of CIW (Manca et al., 2006; Millot, 2014). As the CIW is formed in the Aegean Sea, this
509 intermediate water mass is generally more radiogenic than LIW (Tachikawa et al., 2004; Montagna et al., in
510 prep). Following this hypothesis, a modification of the mixing proportion between the CIW and the LIW may
511 potentially explain values as radiogenic as about -6 in the Sardinia Channel during the Early and Late Holocene
512 (Fig. 5c). However, a stronger LIW and/or a CIW contribution cannot be responsible for ϵNd values as low as -
513 8.66 ± 0.30 observed during the sapropel S1 event at 8.7 ka BP (Table 1, Fig. 5c). Considering that such
514 unradiogenic value is not observed at intermediate depth in the modern eastern Mediterranean basin, the most
515 plausible hypothesis suggested here is that the CWC were ~~bathed-influenced by a higher contribution of~~
516 ~~intermediate water from the western basin in intermediate waters, which were more marked by the western~~
517 ~~basin.~~

518
519

5.3 Hydrological implications for the intermediate water masses of the western Mediterranean Sea

520 The ϵNd records of the Balearic Sea, Alboran Sea and Sardinia Channel document a temporal variability of the
521 east-west gradient in the western Mediterranean basin during the Holocene. The magnitude of the gradient
522 ranges from ~1.5 to ~3 ϵ units during the Early and Late Holocene and it is strongly reduced at 8.7 ka BP
523 coinciding with the sapropel S1 event affecting the eastern Mediterranean basin (Fig. 5). Such variations could

524 be the result of a modification of the Nd isotopic composition of intermediate water masses due to [intensity](#)
525 changes of the ~~the~~ LIW [production](#) through time and a higher contribution of the western-sourced intermediate
526 water towards the Sardinia Channel coinciding with the sapropel S1 event.

527 The LIW acquires its radiogenic ϵNd in the Mediterranean Levantine basin mainly from Nd exchange between
528 seawater and lithogenic particles originating mainly from Nile River (Tachikawa et al., 2004). A higher sediment
529 supply from the Nile River starting at ~15 ka BP was documented by a shift to more radiogenic ϵNd values of
530 the terrigenous fraction obtained from a sediment core having been influenced by the Nile River discharge
531 (Revel et al., 2015) (Fig. 5e). ~~However, Others~~ studies pointed to a gradual enhanced Nile River runoff as soon
532 as 14.8 ka [BP](#) and a peak of Nile discharge from 9.7 to 8.4 ka recorded by large increase in sedimentation rate
533 from 9.7 to 8.4 ka (>120 cm/ka) (Revel et al., 2015; Weldeab et al., 2014; Castaneda et al., 2016). [Similarly,](#)
534 [enhanced Nile discharge at ~9.5 cal kyr B.P. was inferred based on \$\delta^{18}\text{O}\$ in planktonic foraminifera from a](#)
535 [sediment core in the southeast Levantine Basin \(PS009PC \(32°07.7'N, 34°24.4'E; 552 m water depth\)](#)
536 [\(Hennekam et al., 2014\).](#) ~~These~~ [increasing](#) ~~in~~ [contribution of the](#) Nile River ~~discharge to the eastern~~
537 [Mediterranean basin](#) has been related to the African Humid Period (14.8–5.5 ka BP; Shanahan et al., 2015),
538 which in turn was linked to the precessional increase in Northern Hemisphere insolation during low eccentricity
539 (deMenocal et al., 2000; Barker et al., 2004; Garcin et al., 2009). An increasing amount of radiogenic sediments
540 dominated by the Blue/Atbara Nile River contribution (Revel et al., 2014) could have modified the ϵNd of
541 surface water towards more radiogenic values (Revel et al., in prep). [Indeed, planktonic foraminifera \$\epsilon\text{Nd}\$ values](#)
542 [as high as ~ -3 have been documented in the eastern Levantine Basin \(ODP site 967; 34°04.27'N, 32°43.53'E;](#)
543 [2553 m water depth\) during the sapropel S1 event as a result of enhanced Nile flooding \(Scrivner et al., 2004\).](#)
544 ~~This~~ [radiogenic](#) signature was likely transferred to intermediate depth as a consequence of the LIW formation in
545 the Rhodes Gyre, and it might have been propagated westwards towards the Sardinia Channel.

546 ~~The Nile River runoff was also strongly enhanced during the sapropel S1 event (Revel et al., 2010; Weldeab et~~
547 ~~al., 2014; Revel et al., 2014).~~ [Based on \$\delta^{18}\text{O}\$ rube record from a site in the southeast Levantine Basin \(PS009PC](#)
548 [\(32°07.7'N, 34°24.4'E; 552 m water depth\), Hennekam et al. \(2014\) have documented a maximum Nile](#)
549 [discharge at ~9.5 cal kyr B.P., Scrivner et al. \(2004\) have reported very high foraminifera \$\epsilon\text{Nd}\$ values \(-3 to -3.5\)](#)
550 [corresponding to the sapropel S1 event in the eastern Levantine Basin \(ODP site 967; 34°04.27'N, 32°43.53'E;](#)
551 [2553 m water depth\), pointing to a maximum Nile discharge at this time. Hence/Therefore,](#) considering the more
552 unradiogenic value of the CWC samples from the Sardinia Channel during the sapropel S1a event, it is very
553 unlikely that eastern-sourced water flowed at intermediate depth towards the Sardinia Channel. A possible
554 explanation could be the replacement of the radiogenic LIW that was no longer produced in the eastern basin
555 (Rohling, 1994) by less radiogenic western intermediate water (possibly WIW). Such a scenario could even
556 support previous hypotheses ~~that invoke~~ a potential circulation reversal in the eastern Mediterranean from anti-
557 estuarine to estuarine during sapropel formation (Huang and Stanley, 1972; Calvert, 1983; Sarmiento et al.,
558 1988; Buckley and Johnson, 1988; Thunell and Williams, 1989). [An alternative explanation/hypothesis would be](#)
559 [that reduced surface -water densities in the eastern Mediterranean during sapropel S1 resulted in the LIW sinking](#)
560 [to shallower depths during sapropel time than at present. In this case](#)As a result of this shoaling, CWC from the
561 [Sardinia Channel during the sapropel S1a event would have been bathed by underlying wWestern iIntermediate](#)
562 [wWater -during the sapropel S1a event.](#)

Mis en forme : Exosant

Mis en forme : Anglais (États Unis)

564 6. Conclusions

565 The foraminiferal ϵNd record from ~~the~~ intermediate depths in the Balearic Sea reveals a relatively narrow range
566 of ϵNd values varying between -9.50 and -8.61 since the LGM (~20 ka). Between 18 and 13.5 cal ka BP, the
567 more unradiogenic ϵNd values support a vigorous deep overturning in the Gulf of Lions while $\delta^{18}\text{O}$ and $\delta^{13}\text{C}$
568 values indicate a stratification of the water masses after 16 cal ka BP. The stratification together with a decrease
569 of the deep-water intensity led to more radiogenic values after ~13 cal ka BP. The foraminiferal ϵNd record ~~from~~
570 ~~planktonic foraminifera, supplemented-supported by ϵNd values from CWC from the intermediate depths of in~~
571 the Alboran Sea, shows only minor changes in neodymium isotopes ϵNd values from 13.5 cal ka BP to 0.34 cal
572 ka BP, suggesting that the westernmost part of the western Mediterranean basin is not very sensitive to
573 hydrological variations of the LIW.

574 On the contrary, CWC located at the depth of the LIW in the Sardinia Channel ~~indicate-exhibit high~~
575 ~~amplitude~~ large ϵNd variations of the ϵNd values (between -7.75 ± 0.10 and -5.99 ± 0.50) during the Holocene,
576 ~~which could highlight~~ suggesting either the role of the Nile River in changing the ϵNd of the LIW in the eastern
577 Mediterranean basin or a different-variable LIW/CIW mixing of the water outflowing from the Strait of Sicily.
578 ~~Coinciding-At the time of the~~ with the sapropel S1 event at ~8.7 ka BP, CWC display a shift toward lower values
579 (-8.66 ± 0.30), similar to those obtained at intermediate depths in the westernmost part of the western basin. This
580 suggests that western-sourced intermediate water likely filled mid-depth of the southern Sardinia, replacing LIW
581 that was no longer produced (or heavily reduced) in the eastern basin. These results could potentially support a
582 reversal of the Mediterranean circulation, although this assumption needs further investigation to be confirmed.

584 Acknowledgements

585 The research leading to this study has received funding from the French National Research Agency
586 “Investissement d’Avenir” (n°ANR-10-LABX-0018), the HAMOC project ANR-13-BS06-0003, the
587 MISTRALS/PALEOMEX/COFIMED and ENVIMED/Boron Isotope and Trace Elements project. This work
588 contributes to the RITMARE project. We thank Hiske Fink for selecting and kindly providing the cold-water
589 corals samples from the Alboran Sea. We further thank François Thil and Louise Bordier for their support with
590 Nd isotopic composition analyses. Paolo Montagna is grateful for financial support from the Short Term
591 Mobility Program (CNR). Thanks are also extended to the captains, crews, chief scientists, and scientific parties
592 of research cruises RECORD (R/V Urania), POS-385 (R/V Poseidon) and PALEOCINAT II (R/V Le Suroît).

594 References

- 595 Abu-Zied, R. H., Rohling, E. J., Jorissen, F. J., Fontanier, C., Casford, J. S. L. and Cooke, S.: Benthic
596 foraminiferal response to changes in bottom-water oxygenation and organic carbon flux in the eastern
597 Mediterranean during LGM to Recent times, *Mar. Micropaleontol.*, 67(1-2), 46–68,
598 doi:10.1016/j.marmicro.2007.08.006, 2008.
- 599 Allen, J. R. M., Huntley, B., Brandt, U., Brauer, A., Hubberten, H., Keller, J., Kraml, M., Mackensen, A.,
600 Mingram, J., Negendank, J. F. W., Nowaczyk, N. R., Oberhänsli, H., Watts, W. A., Wulf, S. and Zolitschka, B.:
601 Rapid environmental changes in southern Europe during the last glacial period, *Nature*, 400(6746), 740–743,

602 doi:10.1038/23432, 1999.

603 Andersen, M. B., Stirling, C. H., Zimmermann, B. and Halliday, A. N.: Precise determination of the open ocean
604 234U/238U composition, *Geochemistry, Geophys. Geosystems*, 11(12), Q12003, doi:10.1029/2010GC003318,
605 2010.

606 Arsouze, T., Dutay, J.-C., Lacan, F. and Jeandel, C.: Reconstructing the Nd oceanic cycle using a coupled
607 dynamical – biogeochemical model, *Biogeosciences*, 6(12), 2829–2846, doi:10.5194/bg-6-2829-2009, 2009.

608 Astraldi, M., Gasparini, G. P., Gervasio, L. and Salusti, E.: Dense Water Dynamics along the Strait of Sicily
609 (Mediterranean Sea), *J. Phys. Oceanogr.*, 31(12), 3457–3475, doi:10.1175/1520-
610 0485(2001)031<3457:DWDATS>2.0.CO;2, 2001.

611 Astraldi, M., Gasparini, G. P., Vetrano, A. and Vignudelli, S.: Hydrographic characteristics and interannual
612 variability of water masses in the central Mediterranean: A sensitivity test for long-term changes in the
613 Mediterranean Sea, *Deep. Res. Part I Oceanogr. Res. Pap.*, 49(4), 661–680, doi:10.1016/S0967-0637(01)00059-
614 0, 2002a.

615 Astraldi, M., Conversano, F., Civitaresse, G., Gasparini, G. P., Ribera d’Alcalà, M. and Vetrano, a.: Water mass
616 properties and chemical signatures in the central Mediterranean region, *J. Mar. Syst.*, 33-34, 155–177,
617 doi:10.1016/S0924-7963(02)00057-X, 2002b.

618 Bahr, A., Kaboth, S., Jiménez-Espejo, F. J., Sierro, F. J., Voelker, A. H. L., Lourens, L., Röhl, U., Reichert, G.
619 J., Escutia, C., Hernández-Molina, F. J., Pross, J. and Friedrich, O.: Persistent monsoonal forcing of
620 Mediterranean Outflow Water dynamics during the late Pleistocene, *Geology*, 43(11), 951–954,
621 doi:10.1130/G37013.1, 2015.

622 Barker, P. A., Talbot, M. R., Street-Perrott, F. A., Marret, F., Scourse, J. and Odada, E. O.: Late Quaternary
623 climatic variability in intertropical Africa, in *Past Climate Variability through Europe and Africa*, pp. 117–138,
624 Springer Netherlands, Dordrecht., 2004.

625 Bartov, Y., Goldstein, S. L., Stein, M. and Enzel, Y.: Catastrophic arid episodes in the Eastern Mediterranean
626 linked with the North Atlantic Heinrich events, *Geology*, 31(5), 439, doi:10.1130/0091-
627 7613(2003)031<0439:CAEITE>2.0.CO;2, 2003.

628 Bigg, G. R. and Wadley, M. R.: Millennial-scale variability in the oceans: an ocean modelling view, *J. Quat.*
629 *Sci.*, 16(4), 309–319, doi:10.1002/jqs.599, 2001.

630 Bout-Roumazeilles, V., Combourieu-Nebout, N., Desprat, S., Siani, G., Turon, J. L. and Essallami, L.: Tracking
631 atmospheric and riverine terrigenous supplies variability during the last glacial and the Holocene in central
632 Mediterranean, *Clim. Past*, 9(3), 1065–1087, doi:10.5194/cp-9-1065-2013, 2013.

633 Buckley, H. A. and Johnson, L. R.: Late pleistocene to recent sediment deposition in the central and western
634 Mediterranean, *Deep Sea Res. Part A. Oceanogr. Res. Pap.*, 35(5), 749–766, doi:10.1016/0198-0149(88)90028-
635 3, 1988.

636 Cacho, I., Pelejero, C., Grimalt, J. O., Calafat, A. and Canals, M.: C37 alkenone measurements of sea surface
637 temperature in the Gulf of Lions (NW Mediterranean), *Org. Geochem.*, 30(7), 557–566, doi:10.1016/S0146-
638 6380(99)00038-8, 1999.

639 Cacho, I., Grimalt, J. O., Sierro, F. J., Shackleton, N. and Canals, M.: Evidence for enhanced Mediterranean
640 thermohaline circulation during rapid climatic coolings, *Earth Planet. Sci. Lett.*, 183(3-4), 417–429,
641 doi:10.1016/S0012-821X(00)00296-X, 2000.

642 Cacho, I., Grimalt, J. O., Canals, M., Sbaiffi, L., Shackleton, N. J., Schönfeld, J. and Zahn, R.: Variability of the
643 western Mediterranean Sea surface temperature during the last 25,000 years and its connection with the Northern
644 Hemisphere climatic changes, *Paleoceanography*, 16(1), 40–52, doi:10.1029/2000PA000502, 2001.

645 Cacho, I., Grimalt, J. O. and Canals, M.: Response of the Western Mediterranean Sea to rapid climatic variability
646 during the last 50,000 years: a molecular biomarker approach, *J. Mar. Syst.*, 33-34, 253–272,
647 doi:10.1016/S0924-7963(02)00061-1, 2002.

648 Cacho, I., Shackleton, N., Elderfield, H., Sierro, F. J. and Grimalt, J. O.: Glacial rapid variability in deep-water
649 temperature and $\delta^{18}O$ from the Western Mediterranean Sea, *Quat. Sci. Rev.*, 25(23-24), 3294–3311,
650 doi:10.1016/j.quascirev.2006.10.004, 2006.

651 Calvert, S. E.: Geochemistry of Pleistocene sapropels and associated sediments from the Eastern Mediterranean,
652 *Oceanol. Acta*, 6(3), 255–267, 1983.

653 Castañeda, I. S., Schouten, S., Pätzold, J., Lucassen, F., Kasemann, S., Kuhlmann, H. and Schefuß, E.:
654 Hydroclimate variability in the Nile River Basin during the past 28,000 years, *Earth Planet. Sci. Lett.*, 438, 47–
655 56, doi:10.1016/j.epsl.2015.12.014, 2016.

656 Cheng, H., Lawrence Edwards, R., Shen, C.-C., Polyak, V. J., Asmerom, Y., Woodhead, J. D., Hellstrom, J.,
657 Wang, Y., Kong, X., Spötl, C., Wang, X. and Calvin Alexander, E.: Improvements in 230Th dating, 230Th and
658 234U half-life values, and U–Th isotopic measurements by multi-collector inductively coupled plasma mass
659 spectrometry, *Earth Planet. Sci. Lett.*, 371-372, 82–91, doi:10.1016/j.epsl.2013.04.006, 2013.

660 Colin, C., Frank, N., Copard, K. and Douville, E.: Neodymium isotopic composition of deep-sea corals from the
661 NE Atlantic: implications for past hydrological changes during the Holocene, *Quat. Sci. Rev.*, 29(19-20), 2509–
662 2517, doi:10.1016/j.quascirev.2010.05.012, 2010.

663 Combourieu-Nebout, N., Turon, J. L., Zahn, R., Capotondi, L., Londeix, L. and Pahnke, K.: Enhanced aridity
664 and atmospheric high-pressure stability over the western Mediterranean during the North Atlantic cold events of
665 the past 50 k.y, *Geology*, 30(10), 863–866, doi:10.1130/0091-7613(2002)030<0863:EAAAHP>2.0.CO;2, 2002.

666 Copard, K., Colin, C., Douville, E., Freiwald, A., Gudmundsson, G., De Mol, B. and Frank, N.: Nd isotopes in
667 deep-sea corals in the North-eastern Atlantic, *Quat. Sci. Rev.*, 29(19-20), 2499–2508,
668 doi:10.1016/j.quascirev.2010.05.025, 2010.

669 Copard, K., Colin, C., Henderson, G. M., Scholten, J., Douville, E., Sicre, M.-A. and Frank, N.: Late Holocene

670 intermediate water variability in the northeastern Atlantic as recorded by deep-sea corals, *Earth Planet. Sci. Lett.*,
671 313–314, 34–44, doi:10.1016/j.epsl.2011.09.047, 2012.

672 Cramp, A. and O’Sullivan, G.: Neogene sapropels in the Mediterranean: a review, *Mar. Geol.*, 153(1-4), 11–28,
673 doi:10.1016/S0025-3227(98)00092-9, 1999.

674 [De Lange, G. J., Thomson, J., Reitz, A., Slomp, C. P., Principato, M. S., Erba, E. and Corselli, C.: Synchronous](#)
675 [basin-wide formation and redox-controlled preservation of a Mediterranean sapropel, *Nat. Geosci.*, 1\(9\), 606–](#)
676 [610, 2008.](#)

677 DeMenocal, P., Ortiz, J., Guilderson, T. and Sarnthein, M.: Coherent High- and Low-Latitude Climate
678 Variability During the Holocene Warm Period, *Science* (80-.), 288(5474), 2198–2202,
679 doi:10.1126/science.288.5474.2198, 2000.

680 Deschamps, P., Durand, N., Bard, E., Hamelin, B., Camoin, G., Thomas, A. L., Henderson, G. M., Okuno, J. and
681 Yokoyama, Y.: Ice-sheet collapse and sea-level rise at the Bølling warming 14,600 years ago, *Nature*,
682 483(7391), 559–564, doi:10.1038/nature10902, 2012.

683 Douville, E., Sallé, E., Frank, N., Eisele, M., Pons-Branchu, E. and Ayrault, S.: Rapid and accurate U–Th dating
684 of ancient carbonates using inductively coupled plasma-quadrupole mass spectrometry, *Chem. Geol.*, 272(1-4),
685 1–11, doi:10.1016/j.chemgeo.2010.01.007, 2010.

686 Dubois-Dauphin, Q., Colin, C., Bonneau, L., Montagna, P., Wu, Q., Van Rooij, D., Reverdin, G., Douville, E.,
687 Thil, F., Waldner, A., Frank, N.: Fingerprinting North-east Atlantic water masses using Neodymium isotopes,
688 *EPSL*, Submitted.

689

690 Elmore, A. C., Piotrowski, A. M., Wright, J. D. and Scrivner, A. E.: Testing the extraction of past seawater Nd
691 isotopic composition from North Atlantic deep sea sediments and foraminifera, *Geochemistry, Geophys.*
692 *Geosystems*, 12(9), doi:10.1029/2011GC003741, 2011.

693 Emeis, K.-C., Sakamoto, T., Wehausen, R. and Brumsack, H.-J.: The sapropel record of the eastern
694 Mediterranean Sea — results of Ocean Drilling Program Leg 160, *Palaeogeogr. Palaeoclimatol. Palaeoecol.*,
695 158(3-4), 371–395, doi:10.1016/S0031-0182(00)00059-6, 2000.

696 Fink, H. G., Wienberg, C., De Pol-Holz, R., Wintersteller, P. and Hebbeln, D.: Cold-water coral growth in the
697 Alboran Sea related to high productivity during the Late Pleistocene and Holocene, *Mar. Geol.*, 339, 71–82,
698 doi:10.1016/j.margeo.2013.04.009, 2013.

699 Frigola, J., Moreno, A., Cacho, I., Canals, M., Sierro, F. J., Flores, J. a., Grimalt, J. O., Hodell, D. a. and Curtis,
700 J. H.: Holocene climate variability in the western Mediterranean region from a deepwater sediment record,
701 *Paleoceanography*, 22(2), n/a–n/a, doi:10.1029/2006PA001307, 2007.

702 Frigola, J., Moreno, A., Cacho, I., Canals, M., Sierro, F. J., Flores, J. A. and Grimalt, J. O.: Evidence of abrupt
703 changes in Western Mediterranean Deep Water circulation during the last 50kyr: A high-resolution marine
704 record from the Balearic Sea, *Quat. Int.*, 181(1), 88–104, doi:10.1016/j.quaint.2007.06.016, 2008.

- 705 Garcin, Y., Junginger, A., Melnick, D., Olago, D. O., Strecker, M. R. and Trauth, M. H.: Late Pleistocene–
 706 Holocene rise and collapse of Lake Suguta, northern Kenya Rift, *Quat. Sci. Rev.*, 28(9-10), 911–925,
 707 doi:10.1016/j.quascirev.2008.12.006, 2009.
- 708 ~~Grousset, F. E. and Biscaye, P. E.: Tracing dust sources and transport patterns using Sr, Nd and Pb isotopes,
 709 *Chem. Geol.*, 222(3-4), 149–167, doi:10.1016/j.chemgeo.2005.05.006, 2005.~~
- 710 ~~Grousset, F. E., Rognon, P., Coudé-Gaussen, G. and Pédemay, P.: Origins of peri-Saharan dust deposits traced
 711 by their Nd and Sr isotopic composition, *Palaeogeogr. Palaeoclimatol. Palaeoecol.*, 93(3-4), 203–212,
 712 doi:10.1016/0031-0182(92)90097-0, 1992.~~
- 713 ~~Grousset, F. E., Parra, M., Bory, A., Martinez, P., Bertrand, P., Shimmield, G. and Ellam, R. M.: Saharan wind
 714 regimes traced by the Sr Nd isotopic composition of subtropical Atlantic sediments: Last Glacial Maximum vs
 715 today, *Quat. Sci. Rev.*, 17, 395–409, doi:10.1016/S0277-3791(97)00048-6, 1998.~~
- 716 Hebbeln, D., Wienberg, C., Beuck, L., Freiwald, A., Wintersteller, P. and cruise participants (2009) Report and
 717 preliminary results of R/V POSEIDON Cruise 385 "Cold-water corals of the Alboran Sea (western
 718 Mediterranean Sea)", Faro - Toulon, 29.5. - 16.6.2009. Reports of the Department of Geosciences at the
 719 University of Bremen, No. 273. Department of Geosciences, Bremen University. urn:nbn:de:gbv:46-
 720 ep000106508.
- 721 ~~Hennekam, R., Jilbert, T., Schnetger, B. and De Lange, G. J.: Solar forcing of Nile discharge and sapropel S1
 722 formation in the early to middle Holocene eastern Mediterranean, *Paleoceanography*, 29(5), 343–356,
 723 doi:10.1002/2013PA002553, 2014.~~
- 724 Henry, F., Jeandel, C., Dupré, B. and Minster, J.-F.: Particulate and dissolved Nd in the western Mediterranean
 725 Sea: Sources, fate and budget, *Mar. Chem.*, 45(4), 283–305, doi:10.1016/0304-4203(94)90075-2, 1994.
- 726 Hooghiemstra, H., Bechler, A. and Beug, H.-J.: Isopollen maps for 18,000 years B.P. of the Atlantic offshore of
 727 northwest Africa: Evidence for paleowind circulation, *Paleoceanography*, 2, 561–582,
 728 doi:10.1029/PA002i006p00561, 1987.
- 729 Hopkins, T. S.: Recent observations on the intermediate and deep water circulation in the Southern Tyrrhenian
 730 Sea, *Oceanol. Acta*, (Special issue), 41–50, 1988.
- 731 Huang, T. C. and Stanley, D. J.: Western Alboran sea: sediment dispersal, ponding and reversal of currents, in
 732 *The Mediterranean Sea: A Natural Sedimentation Laboratory*, pp. 521–559, Dowden, Hutchinson & Ross,
 733 Stroudsburg, PA., 1972.
- 734 Hutson, W. H.: The Agulhas Current During the Late Pleistocene: Analysis of Modern Faunal Analogs, *Science*
 735 (80-.), 207(4426), 64–66, doi:10.1126/science.207.4426.64, 1980.
- 736 Itambi, a. C., von Dobeneck, T., Mulitza, S., Bickert, T. and Heslop, D.: Millennial-scale northwest African
 737 droughts related to Heinrich events and Dansgaard-Oeschger cycles: Evidence in marine sediments from
 738 offshore Senegal, *Paleoceanography*, 24(1), PA1205, doi:10.1029/2007PA001570, 2009.

Mis en forme : Anglais (Royaume-Uni)

- 739 Ivy-Ochs, S., Kerschner, H. and Schlüchter, C.: Cosmogenic nuclides and the dating of Lateglacial and Early
740 Holocene glacier variations: The Alpine perspective, *Quat. Int.*, 164-165, 53–63,
741 doi:10.1016/j.quaint.2006.12.008, 2007.
- 742 Jacobsen, S. B. and Wasserburg, G. J.: Sm-Nd isotopic evolution of chondrites, *Earth Planet. Sci. Lett.*, 50(1),
743 139–155, doi:10.1016/0012-821X(80)90125-9, 1980.
- 744 Jaffey, A. H., Flynn, K. F., Glendenin, L. E., Bentley, W. C. and Essling, A. M.: Precision measurements of half-
745 lives and specific activities of ²³⁵U and ²³⁸U, *Phys. Rev. C*, 4(5), 1889–1906, doi:10.1103/PhysRevC.4.1889,
746 1971.
- 747 Jiménez-Espejo, F. J., Pardos-Gené, M., Martínez-Ruiz, F., García-Alix, A., van de Flierdt, T., Toyofuku, T.,
748 Bahr, A. and Kreissig, K.: Geochemical evidence for intermediate water circulation in the westernmost
749 Mediterranean over the last 20kyrBP and its impact on the Mediterranean Outflow, *Glob. Planet. Change*, 135,
750 38–46, doi:10.1016/j.gloplacha.2015.10.001, 2015.
- 751 Kallel, N., Paterne, M., Labeyrie, L., Duplessy, J.-C. and Arnold, M.: Temperature and salinity records of the
752 Tyrrhenian Sea during the last 18,000 years, *Palaeogeogr. Palaeoclimatol. Palaeoecol.*, 135(1-4), 97–108,
753 doi:10.1016/S0031-0182(97)00021-7, 1997.
- 754 Kelly, M. A., Ivy-Ochs, S., Kubik, P. W., Von Blanckenburg, F. and Schlüchter, C.: Chronology of deglaciation
755 based on ¹⁰Be dates of glacial erosional features in the Grimsel Pass region, central Swiss Alps, *Boreas*, 35(4),
756 634–643, doi:10.1111/j.1502-3885.2006.tb01169.x, 2006.
- 757 Khelifi, N., Samthein, M., Andersen, N., Blanz, T., Frank, M., Garbe-Schonberg, D., Haley, B. a., Stumpf, R.
758 and Weinelt, M.: A major and long-term Pliocene intensification of the Mediterranean outflow, 3.5-3.3 Ma ago,
759 *Geology*, 37(9), 811–814, doi:10.1130/G30058A.1, 2009.
- 760 Kinder, T. H. and Parrilla, G.: Yes, some of the Mediterranean water does come from great depth, *J. Geophys.*
761 *Res.*, 92, 2901–2906, doi:10.1029/JC092iC03p02901, 1987.
- 762 Kuhnt, T., Schmiedl, G., Ehrmann, W., Hamann, Y. and Hemleben, C.: Deep-sea ecosystem variability of the
763 Aegean Sea during the past 22 kyr as revealed by Benthic Foraminifera, *Mar. Micropaleontol.*, 64(3-4), 141–
764 162, doi:10.1016/j.marmicro.2007.04.003, 2007.
- 765 Kuhnt, T., Schmiedl, G., Ehrmann, W., Hamann, Y. and Andersen, N.: Stable isotopic composition of Holocene
766 benthic foraminifers from the Eastern Mediterranean Sea: Past changes in productivity and deep water
767 oxygenation, *Palaeogeogr. Palaeoclimatol. Palaeoecol.*, 268(1-2), 106–115, doi:10.1016/j.palaeo.2008.07.010,
768 2008.
- 769 Lacan, F. and Jeandel, C.: Tracing Papua New Guinea imprint on the central Equatorial Pacific Ocean using
770 neodymium isotopic compositions and Rare Earth Element patterns, *Earth Planet. Sci. Lett.*, 186(3-4), 497–512,
771 doi:10.1016/S0012-821X(01)00263-1, 2001.
- 772 Lacan, F. and Jeandel, C.: Neodymium isotopes as a new tool for quantifying exchange fluxes at the continent–

773 ocean interface, *Earth Planet. Sci. Lett.*, 232(3-4), 245–257, doi:10.1016/j.epsl.2005.01.004, 2005.

774 Lascaratos, A. and Nittis, K.: A high-resolution three-dimensional numerical study of intermediate water
775 formation in the Levantine Sea, *J. Geophys. Res.*, 103(C9), 18497, doi:10.1029/98JC01196, 1998.

776 Lascaratos, A., Williams, R. G. and Tragou, E.: A mixed-layer study of the formation of Levantine intermediate
777 water, *J. Geophys. Res.*, 98(C8), 14739, doi:10.1029/93JC00912, 1993.

778 López Correa, M., Montagna, P., Joseph, N., Rüggeberg, A., Fietzke, J., Flögel, S., Dorschel, B., Goldstein, S.
779 L., Wheeler, A. and Freiwald, A.: Preboreal onset of cold-water coral growth beyond the Arctic Circle revealed
780 by coupled radiocarbon and U-series dating and neodymium isotopes, *Quat. Sci. Rev.*, 34, 24–43,
781 doi:10.1016/j.quascirev.2011.12.005, 2012.

782 López-Jurado, J. L., Marcos, M. and Monserrat, S.: Hydrographic conditions affecting two fishing grounds of
783 Mallorca island (Western Mediterranean): during the IDEA Project (2003-2004), *J. Mar. Syst.*, 71(3-4), 303–
784 315, doi:10.1016/j.jmarsys.2007.03.007, 2008.

785 Ludwig, K. R. and Titterton, D. M.: Calculation of $^{230}\text{Th}/\text{U}$ isochrons, ages, and errors, *Geochim.*
786 *Cosmochim. Acta*, 58(22), 5031–5042, doi:http://dx.doi.org/10.1016/0016-7037(94)90229-1, 1994.

787 Lugmair, G. W., Shimamura, T., Lewis, R. S. and Anders, E.: Samarium-146 in the Early Solar System:
788 Evidence from Neodymium in the Allende Meteorite, *Science* (80-.), 222(4627), 1015–1018,
789 doi:10.1126/science.222.4627.1015, 1983.

790 Malanotte-Rizzoli, P., Manca, B. B., D'Alcala, M. R., Theocharis, A., Brenner, S., Budillon, G. and Ozsoy, E.:
791 The Eastern Mediterranean in the 80s and in the 90s: the big transition in the intermediate and deep circulations,
792 *Dyn. Atmos. Ocean.*, 29(2-4), 365–395, doi:10.1016/S0377-0265(99)00011-1, 1999.

793 Manca, B., Ibello, V., Pacciaroni, M., Scarazzato, P. and Giorgetti, A.: Ventilation of deep waters in the Adriatic
794 and Ionian Seas following changes in thermohaline circulation of the Eastern Mediterranean, *Clim. Res.*, 31,
795 239–256, doi:10.3354/cr031239, 2006.

796 Martrat, B., Grimalt, J. O., Lopez-Martinez, C., Cacho, I., Sierro, F. J., Flores, J. A., Zahn, R., Canals, M.,
797 Curtis, J. H. and Hodell, D. a: Abrupt temperature changes in the Western Mediterranean over the past 250,000
798 years., *Science* (80-.), 306(5702), 1762–1765, doi:10.1126/science.1101706, 2004.

799 [Martrat, B., Jimenez-Amat, P., Zahn, R. and Grimalt, J. O.: Similarities and dissimilarities between the last two
800 deglaciations and interglaciations in the North Atlantic region, *Quat. Sci. Rev.*, 99, 122–134,
801 doi:10.1016/j.quascirev.2014.06.016, 2014.](#)

802 Melki, T., Kallel, N., Jorissen, F. J., Guichard, F., Dennielou, B., Berné, S., Labeyrie, L. and Fontugne, M.:
803 Abrupt climate change, sea surface salinity and paleoproductivity in the western Mediterranean Sea (Gulf of
804 Lion) during the last 28 kyr, *Palaeogeogr. Palaeoclimatol. Palaeoecol.*, 279(1-2), 96–113,
805 doi:10.1016/j.palaeo.2009.05.005, 2009.

806

- 807 Mercone, D., Thomson, J., Croudace, I. W., Siani, G., Paterne, M. and Troelstra, S.: Duration of S1, the most
808 recent sapropel in the eastern Mediterranean Sea, as indicated by accelerator mass spectrometry radiocarbon and
809 geochemical evidence, *Paleoceanography*, 15(3), 336–347, doi:10.1029/1999PA000397, 2000.
- 810 Mercone, D., Thomson, J., Abu-Zied, R. H., Croudace, I. W. and Rohling, E. J.: High-resolution geochemical
811 and micropalaeontological profiling of the most recent eastern Mediterranean sapropel, *Mar. Geol.*, 177(1-2),
812 25–44, doi:10.1016/S0025-3227(01)00122-0, 2001.
- 813 Millot, C.: Circulation in the Western Mediterranean Sea, *J. Mar. Syst.*, 20(1-4), 423–442, doi:10.1016/S0924-
814 7963(98)00078-5, 1999.
- 815 Millot, C.: Another description of the Mediterranean Sea outflow, *Prog. Oceanogr.*, 82(2), 101–124,
816 doi:10.1016/j.pocean.2009.04.016, 2009.
- 817 Millot, C.: Heterogeneities of in- and out-flows in the Mediterranean Sea, *Prog. Oceanogr.*, 120, 254–278,
818 doi:10.1016/j.pocean.2013.09.007, 2014.
- 819 Millot, C. and Taupier-Letage, I.: Circulation in the Mediterranean Sea, in *Environmental Chemistry*, vol. 5,
820 edited by A. Saliot, pp. 29–66, Springer Berlin Heidelberg, Heidelberg., 2005.
- 821 Millot, C., Candela, J., Fuda, J.-L. and Tber, Y.: Large warming and salinification of the Mediterranean outflow
822 due to changes in its composition, *Deep Sea Res. Part I Oceanogr. Res. Pap.*, 53(4), 656–666,
823 doi:10.1016/j.dsr.2005.12.017, 2006.
- 824 Montero-Serrano, J.-C., Frank, N., Colin, C., Wienberg, C. and Eisele, M.: The climate influence on the mid-
825 depth Northeast Atlantic gyres viewed by cold-water corals, *Geophys. Res. Lett.*, 38(19),
826 doi:10.1029/2011GL048733, 2011.
- 827 Montero-Serrano, J.-C., Frank, N., Tisnérat-Laborde, N., Colin, C., Wu, C., Lin, K., Shen, C., Copard, K.,
828 Orejas, C., Gori, A., De Mol, L., Van Rooij, D., Reverdin, G. and Douville, E.: Decadal changes in the mid-
829 depth water mass dynamic of the Northeastern Atlantic margin (Bay of Biscay), *Earth Planet. Sci. Lett.*, 364,
830 134–144, doi:10.1016/j.epsl.2013.01.012, 2013.
- 831 Moreno, A., Cacho, I., Canals, M., Prins, M. a., Sánchez-Goñi, M.-F., Grimal, O. J. and Weltje, G. J.: Saharan
832 Dust Transport and High-Latitude Glacial Climatic Variability: The Alboran Sea Record, *Quat. Res.*, 58, 318–
833 328, doi:10.1006/qres.2002.2383, 2002.
- 834 Moreno, A., Cacho, I., Canals, M., Grimalt, J. O., Sánchez-Goñi, M. F., Shackleton, N. and Sierro, F. J.: Links
835 between marine and atmospheric processes oscillating on a millennial time-scale. A multi-proxy study of the last
836 50,000yr from the Alboran Sea (Western Mediterranean Sea), *Quat. Sci. Rev.*, 24(14-15), 1623–1636,
837 doi:10.1016/j.quascirev.2004.06.018, 2005.
- 838 [Myers, P. G., Haines, K. and Rohling, E. J.: Modeling the paleocirculation of the Mediterranean: The Last](#)
839 [Glacial Maximum and the Holocene with emphasis on the formation of sapropel S1, *Paleoceanography*, 13\(6\),](#)
840 [586–606, doi:10.1029/98PA02736, 1998.](#)

Mis en forme : Anglais (Royaume-Uni)

- 841 Ovchinnikov, I. M.: The formation of intermediate water in the Mediterranean, *Oceanology*, 24, 168–173, 1984.
- 842 Overpeck, J. T., Webb, T. and Prentice, I. C.: Quantitative interpretation of fossil pollen spectra: Dissimilarity
843 coefficients and the method of modern analogs, *Quat. Res.*, 23(1), 87–108, doi:10.1016/0033-5894(85)90074-2,
844 1985.
- 845 Paterne, M., Kallel, N., Labeyrie, L., Vautravers, M., Duplessy, J.-C., Rossignol-Strick, M., Cortijo, E., Arnold,
846 M. and Fontugne, M.: Hydrological relationship between the North Atlantic Ocean and the Mediterranean Sea
847 during the past 15-75 kyr, *Paleoceanography*, 14(5), 626–638, doi:10.1029/1998PA900022, 1999.
- 848 Pérez-Folgado, M., Sierro, F. J., Flores, J. A., Cacho, I., Grimalt, J. O., Zahn, R. and Shackleton, N.: Western
849 Mediterranean planktonic foraminifera events and millennial climatic variability during the last 70 kyr, *Mar.*
850 *Micropaleontol.*, 48(1-2), 49–70, doi:10.1016/S0377-8398(02)00160-3, 2003.
- 851 Pinardi, N. and Masetti, E.: Variability of the large scale general circulation of the Mediterranean Sea from
852 observations and modelling: a review, *Palaeogeogr. Palaeoclimatol. Palaeoecol.*, 158(3-4), 153–173,
853 doi:10.1016/S0031-0182(00)00048-1, 2000.
- 854 Piotrowski, A. M., Galy, A., Nicholl, J. a. L., Roberts, N. L., Wilson, D. J., Clegg, J. a. and Yu, J.:
855 Reconstructing deglacial North and South Atlantic deep water sourcing using foraminiferal Nd isotopes, *Earth*
856 *Planet. Sci. Lett.*, 357-358, 289–297, doi:10.1016/j.epsl.2012.09.036, 2012.
- 857 Pons-Branchu, E., Douville, E., Roy-Barman, M., Dumont, E., Branchu, P., Thil, F., Frank, N., Bordier, L. and
858 Borst, W.: A geochemical perspective on Parisian urban history based on U–Th dating, laminae counting and
859 yttrium and REE concentrations of recent carbonates in underground aqueducts, *Quat. Geochronol.*, 24, 44–53,
860 doi:10.1016/j.quageo.2014.08.001, 2014.
- 861 Prell, W. L.: Stability of low-latitude sea-surface temperatures: an evaluation of the CLIMAP reconstruction
862 with emphasis on the positive SST anomalies. Final report, Providence, RI (USA)., 1985.
- 863 Reimer, P. J., Bard, E., Bayliss, A., Beck, J. W., Blackwell, P. G., Bronk Ramsey, C., Grootes, P. M.,
864 Guilderson, T. P., Hafliðason, H., Hajdas, I., HattĹ, C., Heaton, T. J., Hoffmann, D. L., Hogg, A. G., Hughen, K.
865 A., Kaiser, K. F., Kromer, B., Manning, S. W., Niu, M., Reimer, R. W., Richards, D. A., Scott, E. M., Southon,
866 J. R., Staff, R. A., Turney, C. S. M., & van der Plicht, J. (2013). IntCal13 and Marine13 Radiocarbon Age
867 Calibration Curves 0-50,000 Years cal BP. *Radiocarbon*, 55(4).
- 868 ~~Revel, M., Ducassou, E., Grousset, F. E., Bernasconi, S., Migeon, S., Revillon, S., Mascle, J., Murat, A.,~~
869 ~~Zaragosi, S. and Bosch, D.: 100,000 Years of African monsoon variability recorded in sediments of the Nile~~
870 ~~margin, *Quat. Sci. Rev.*, 29(11-12), 1342–1362, doi:10.1016/j.quascirev.2010.02.006, 2010.~~
- 871 Revel, M., Colin, C., Bernasconi, S., Combourieu-Nebout, N., Ducassou, E., Grousset, F. E., Rolland, Y.,
872 Migeon, S., Bosch, D., Brunet, P., Zhao, Y. and Mascle, J.: 21,000 Years of Ethiopian African monsoon
873 variability recorded in sediments of the western Nile deep-sea fan, *Reg. Environ. Chang.*, 14(5), 1685–1696,
874 doi:10.1007/s10113-014-0588-x, 2014.

875 Revel, M., Ducassou, E., Skonieczny, C., Colin, C., Bastian, L., Bosch, D., Migeon, S. and Mascle, J.: 20,000
876 years of Nile River dynamics and environmental changes in the Nile catchment area as inferred from Nile upper
877 continental slope sediments, *Quat. Sci. Rev.*, 130, 200–221, doi:10.1016/j.quascirev.2015.10.030, 2015.

878 Roberts, N. L., Piotrowski, A. M., McManus, J. F. and Keigwin, L. D.: Synchronous deglacial overturning and
879 water mass source changes., *Science*, 327(2010), 75–78, doi:10.1126/science.1178068, 2010.

880 [Rodrigo-Gámiz, M., Martínez-Ruiz, F., Rampen, S. W., Schouten, S. and Sinninghe Damsté, J. S.: Sea surface](#)
881 [temperature variations in the western Mediterranean Sea over the last 20 kyr: A dual-organic proxy \(U K' 37 and](#)
882 [LDI\) approach, *Paleoceanography*, 29\(2\), 87–98, doi:10.1002/2013PA002466, 2014.](#)

883 [Rodrigo-Gámiz, M., Martínez-Ruiz, F., Chiaradia, M., Jiménez-Espejo, F. J. and Ariztegui, D.: Radiogenic](#)
884 [isotopes for deciphering terrigenous input provenance in the western Mediterranean, *Chem. Geol.*, 410, 237–250,](#)
885 [doi:10.1016/j.chemgeo.2015.06.004, 2015.](#)

886 Rogerson, M., Rohling, E. J., Weaver, P. P. E. and Murray, J. W.: Glacial to interglacial changes in the settling
887 depth of the Mediterranean Outflow plume, *Paleoceanography*, 20(3), doi:10.1029/2004PA001106, 2005.

888 Rogerson, M., Rohling, E. J. and Weaver, P. P. E.: Promotion of meridional overturning by Mediterranean-
889 derived salt during the last deglaciation, *Paleoceanography*, 21(4), 1–8, doi:10.1029/2006PA001306, 2006.

890 Rogerson, M., Cacho, I., Jimenez-Espejo, F., Reguera, M. I., Sierro, F. J., Martinez-Ruiz, F., Frigola, J. and
891 Canals, M.: A dynamic explanation for the origin of the western Mediterranean organic-rich layers,
892 *Geochemistry, Geophys. Geosystems*, 9(7), n/a–n/a, doi:10.1029/2007GC001936, 2008.

893 Rohling, E. J.: Review and new aspects concerning the formation of eastern Mediterranean sapropels, *Mar.*
894 *Geol.*, 122(1-2), 1–28, doi:10.1016/0025-3227(94)90202-X, 1994.

895 Rohling, E. J., Jorissen, F. J. and De stigter, H. C.: 200 Year interruption of Holocene sapropel formation in the
896 Adriatic Sea, *J. Micropalaeontology*, 16(2), 97–108, doi:10.1144/jm.16.2.97, 1997.

897 Rohling, E. J., Mayewski, P. a, Abu-Zied, R. H., Casford, J. S. L. and Hayes, A.: Holocene atmosphere-ocean
898 interactions: records from Greenland and the Aegean Sea, *Clim. Dyn.*, 18(7), 587–593, doi:10.1007/s00382-001-
899 0194-8, 2002.

900 Rohling, E. J., Sprovieri, M., Cane, T., Casford, J. S. ., Cooke, S., Bouloubassi, I., Emeis, K. C., Schiebel, R.,
901 Rogerson, M., Hayes, A., Jorissen, F. . and Kroon, D.: Reconstructing past planktic foraminiferal habitats using
902 stable isotope data: a case history for Mediterranean sapropel S5, *Mar. Micropaleontol.*, 50(1-2), 89–123,
903 doi:10.1016/S0377-8398(03)00068-9, 2004.

904 Rohling, E. J., Marino, G. and Grant, K. M.: Mediterranean climate and oceanography, and the periodic
905 development of anoxic events (sapropels), *Earth-Science Rev.*, 143, 62–97, doi:10.1016/j.earscirev.2015.01.008,
906 2015.

907 Rossignol-Strick, M., Nesteroff, W., Olive, P. and Vergnaud-Grazzini, C.: After the deluge: Mediterranean

- 908 stagnation and sapropel formation, *Nature*, 295(5845), 105–110, doi:10.1038/295105a0, 1982.
- 909 Sammari, C., Millot, C., Taupier-Letage, I., Stefani, A. and Brahim, M.: Hydrological characteristics in the
910 Tunisia–Sardinia–Sicily area during spring 1995, *Deep Sea Res. Part I Oceanogr. Res. Pap.*, 46(10), 1671–1703,
911 doi:10.1016/S0967-0637(99)00026-6, 1999.
- 912 Sarmiento, J. L., Herbert, T. and Toggweiler, J. R.: Mediterranean nutrient balance and episodes of anoxia,
913 *Global Biogeochem. Cycles*, 2(4), 427–444, doi:10.1029/GB002i004p00427, 1988.
- 914
- 915 Sánchez-Goñi, M., Cacho, I., Turon, J. L., Guiot, J., Sierro, F. J., Peypouquet, J., Grimalt, J. O. and Shackleton,
916 N. J.: Synchronicity between marine and terrestrial responses to millennial scale climatic variability during the
917 last glacial period in the Mediterranean region, *Clim. Dyn.*, 19(1), 95–105, doi:10.1007/s00382-001-0212-x,
918 2002.
- 919 Sarnthein, M., Tetzlaff, G., Koopmann, B., Wolter, K. and Pflaumann, U.: Glacial and interglacial wind regimes
920 over the eastern subtropical Atlantic and North-West Africa, *Nature*, 293, 193–196, doi:10.1038/293193a0,
921 1981.
- 922 [Scheuvens, D., Schütz, L., Kandler, K., Ebert, M. and Weinbruch, S.: Bulk composition of northern African dust](#)
923 [and its source sediments — A compilation, *Earth-Science Rev.*, 116, 170–194,](#)
924 [doi:10.1016/j.earscirev.2012.08.005, 2013.](#)
- 925 Schmiedl, G., Kuhnt, T., Ehrmann, W., Emeis, K. C., Hamann, Y., Kotthoff, U., Dulski, P. and Pross, J.:
926 Climatic forcing of eastern Mediterranean deep-water formation and benthic ecosystems during the past 22 000
927 years, *Quat. Sci. Rev.*, 29(23-24), 3006–3020, doi:10.1016/j.quascirev.2010.07.002, 2010.
- 928 Schönfeld, J. and Zahn, R.: Late Glacial to Holocene history of the Mediterranean outflow. Evidence from
929 benthic foraminiferal assemblages and stable isotopes at the Portuguese margin, *Palaeogeogr. Palaeoclimatol.*
930 *Palaeoecol.*, 159(1-2), 85–111, doi:10.1016/S0031-0182(00)00035-3, 2000.
- 931 Schott, F., Visbeck, M., Send, U., Fischer, J., Stramma, L. and Desaubies, Y.: Observations of Deep Convection
932 in the Gulf of Lions, Northern Mediterranean, during the Winter of 1991/92, *J. Phys. Oceanogr.*, 26(4), 505–524,
933 doi:10.1175/1520-0485(1996)026<0505:ODCIT>2.0.CO;2, 1996.
- 934 Schroeder, K., Millot, C., Bengara, L., Ben Ismail, S., Bensi, M., Borghini, M., Budillon, G., Cardin, V.,
935 Coppola, L., Curtil, C., Drago, A., El Moumni, B., Font, J., Fuda, J. L., García-Lafuente, J., Gasparini, G. P.,
936 Kontoyiannis, H., Lefevre, D., Puig, P., Raimbault, P., Rougier, G., Salat, J., Sammari, C., Sánchez Garrido, J.
937 C., Sanchez-Roman, A., Sparnocchia, S., Tamburini, C., Taupier-Letage, I., Theocharis, A., Vargas-Yáñez, M.
938 and Vetrano, A.: Long-term monitoring programme of the hydrological variability in the Mediterranean Sea: a
939 first overview of the HYDROCHANGES network, *Ocean Sci.*, 9(2), 301–324, doi:10.5194/os-9-301-2013,
940 2013.
- 941 Scrivner, A. E., Vance, D. and Rohling, E. J.: New neodymium isotope data quantify Nile involvement in
942 Mediterranean anoxic episodes, *Geology*, 32(7), 565, doi:10.1130/G20419.1, 2004.

Mis en forme : Anglais (Royaume-Uni)

943 Shanahan, T. M., McKay, N. P., Hughen, K. A., Overpeck, J. T., Otto-Bliesner, B., Heil, C. W., King, J., Scholz,
944 C. A. and Peck, J.: The time-transgressive termination of the African Humid Period, *Nat. Geosci.*, 8(2), 140–144,
945 doi:10.1038/ngeo2329, 2015.

946 Siani, G., Paterne, M., Arnold, M., Bard, E., Metivier, B., Tisnerat, N. and Bassinot, F.: Radiocarbon reservoir
947 ages in the Mediterranean Sea and Black Sea, *Radiocarbon*, 42(2), 271–280 [online] Available from: <Go to
948 ISI>://000089971000010, 2000.

949 Siani, G., Paterne, M., Michel, E., Sulpizio, R., Sbrana, A., Arnold, M. and Haddad, G.: Mediterranean Sea
950 surface radiocarbon reservoir age changes since the last glacial maximum., *Science* (80-.), 294(5548), 1917–
951 1920, doi:10.1126/science.1063649, 2001.

952 Siani, G., Sulpizio, R., Paterne, M. and Sbrana, A.: Tephrostratigraphy study for the last 18,000 C years in a
953 deep-sea sediment sequence for the South Adriatic, *Quat. Sci. Rev.*, 23(23-24), 2485–2500,
954 doi:10.1016/j.quascirev.2004.06.004, 2004.

955 Siani, G., Magny, M., Paterne, M., Debret, M., Fontugne, M. (2013) - Paleohydrology reconstruction and
956 Holocene climate variability in the South Adriatic Sea. *Climate of the Past*, 9, 499-515.

957 Sierro, F. J., Hodell, D. A., Curtis, J. H., Flores, J. A., Reguera, I., Colmenero-Hidalgo, E., Bárcena, M. A.,
958 Grimalt, J. O., Cacho, I., Frigola, J. and Canals, M.: Impact of iceberg melting on Mediterranean thermohaline
959 circulation during Heinrich events, *Paleoceanography*, 20(2), n/a–n/a, doi:10.1029/2004PA001051, 2005.

960 Sparnocchia, S., Gasparini, G. P., Astraldi, M., Borghini, M. and Pistek, P.: Dynamics and mixing of the Eastern
961 Mediterranean outflow in the Tyrrhenian basin, *J. Mar. Syst.*, 20(1-4), 301–317, doi:10.1016/S0924-
962 7963(98)00088-8, 1999.

963 Spivack, A. J. and Wasserburg, G. J.: Neodymium isotopic composition of the Mediterranean outflow and the
964 eastern North Atlantic, *Geochim. Cosmochim. Acta*, 52(12), 2767–2773, doi:10.1016/0016-7037(88)90144-5,
965 1988.

966 [Stratford, K., Williams, R. G. and Myers, P. G.: Impact of the circulation on Sapropel Formation in the eastern](#)
967 [Mediterranean, *Global Biogeochem. Cycles*, 14\(2\), 683–695, doi:10.1029/1999GB001157, 2000.](#)

968 Stuiver, M., Reimer, P. J. and Reimer, R.: CALIB 7.0, *Radiocarb. Calibration Progr.*, 2005.

969 Tachikawa, K., Roy-Barman, M., Michard, A., Thouron, D., Yeghicheyan, D. and Jeandel, C.: Neodymium
970 isotopes in the Mediterranean Sea: comparison between seawater and sediment signals, *Geochim. Cosmochim.*
971 *Acta*, 68(14), 3095–3106, doi:10.1016/j.gca.2004.01.024, 2004.

972 Tachikawa, K., Piotrowski, A. M. and Bayon, G.: Neodymium associated with foraminiferal carbonate as a
973 recorder of seawater isotopic signatures, *Quat. Sci. Rev.*, 88, 1–13, doi:10.1016/j.quascirev.2013.12.027, 2014.

974 Tanaka, T., Togashi, S., Kamioka, H., Amakawa, H., Kagami, H., Hamamoto, T., Yuhara, M., Orihashi, Y.,
975 Yoneda, S., Shimizu, H., Kunimaru, T., Takahashi, K., Yanagi, T., Nakano, T., Fujimaki, H., Shinjo, R.,
976 Asahara, Y., Tanimizu, M. and Dragusanu, C.: JNdi-1: a neodymium isotopic reference in consistency with

977 LaJolla neodymium, *Chem. Geol.*, 168(3-4), 279–281, doi:10.1016/S0009-2541(00)00198-4, 2000.

978 Tachikawa, K., Vidal, L., Cornuault, M., Garcia, M., Pothin, A., Sonzogni, C., Bard, E., Menot, G. and Revel,
979 M.: Eastern Mediterranean Sea circulation inferred from the conditions of S1 sapropel deposition, *Clim. Past*,
980 11(6), 855–867, doi:10.5194/cp-11-855-2015, 2015.

981 Taviani, M., Angeletti, L., Canese, S., Cannas, R., Cardone, F., Cau, A., Cau, A. B., Follesa, M. C., Marchese,
982 F., Montagna, P. and Tessarolo, C.: The “Sardinian cold-water coral province” in the context of the
983 Mediterranean coral ecosystems, *Deep Sea Res. Part II Top. Stud. Oceanogr.*, doi:10.1016/j.dsr2.2015.12.008,
984 2015.

985 Thunell, R. C. and Williams, D. F.: Glacial–Holocene salinity changes in the Mediterranean Sea: hydrographic
986 and depositional effects, *Nature*, 338(6215), 493–496, doi:10.1038/338493a0, 1989.

987 Toucanne, S., Jouet, G., Ducassou, E., Bassetti, M. A., Dennielou, B., Angue Minto’o, C. M., Lahmi, M.,
988 Touyet, N., Charlier, K., Lericolais, G. and Mulder, T.: A 130,000-year record of Levantine Intermediate Water
989 flow variability in the Corsica Trough, western Mediterranean Sea, *Quat. Sci. Rev.*, 33, 55–73,
990 doi:10.1016/j.quascirev.2011.11.020, 2012.

991 Vance, D., Scrivner, A. E. and Beney, P.: The use of foraminifera as a record of the past neodymium isotope
992 composition of seawater, *Paleoceanography*, 19(2), PA2009, doi:10.1029/2003PA000957, 2004.

993 van de Flierdt, T., Robinson, L. F. and Adkins, J. F.: Deep-sea coral aragonite as a recorder for the neodymium
994 isotopic composition of seawater, *Geochim. Cosmochim. Acta*, 74(21), 6014–6032,
995 doi:10.1016/j.gca.2010.08.001, 2010.

996 Voelker, A. H. L., Lebreiro, S. M., Schönfeld, J., Cacho, I., Erlenkeuser, H. and Abrantes, F.: Mediterranean
997 outflow strengthening during northern hemisphere coolings: A salt source for the glacial Atlantic?, *Earth Planet.*
998 *Sci. Lett.*, 245, 39–55, doi:10.1016/j.epsl.2006.03.014, 2006.

999 Weaver, A. J., Saenko, O. a., Clark, P. U. and Mitrovica, J. X.: Meltwater Pulse 1A from Antarctica as a Trigger
1000 of the Bolling-Allerod Warm Interval, *Science* (80-.), 299(5613), 1709–1713, doi:10.1126/science.1081002,
1001 2003.

1002 Weldeab, S., Emeis, K.-C., Hemleben, C. and Siebel, W.: Provenance of lithogenic surface sediments and
1003 pathways of riverine suspended matter in the Eastern Mediterranean Sea: evidence from $^{143}\text{Nd}/^{144}\text{Nd}$ and
1004 $^{87}\text{Sr}/^{86}\text{Sr}$ ratios, *Chem. Geol.*, 186(1-2), 139–149, doi:10.1016/S0009-2541(01)00415-6, 2002.

1005 Weldeab, S., Menke, V. and Schmiedl, G.: The pace of East African monsoon evolution during the Holocene,
1006 *Geophys. Res. Lett.*, 41, 1724–1731, doi:10.1002/2014GL059361.Received, 2014.

1007 Wienberg, C., Frank, N., Mertens, K. N., Stuut, J.-B. W., Marchant, M., Fietzke, J., Mienis, F. and Hebbeln, D.:
1008 Glacial cold-water coral growth in the Gulf of Cádiz: Implications of increased palaeo-productivity, *Earth*
1009 *Planet. Sci. Lett.*, 298(3-4), 405–416, doi:10.1016/j.epsl.2010.08.017, 2010.

1010 Wu, Q., Colin, C., Liu, Z., Thil, F., Dubois-Dauphin, Q., Frank, N., Tachikawa, K., Bordier, L. and Douville, E.:
1011 Neodymium isotopic composition in foraminifera and authigenic phases of the South China Sea sediments:
1012 Implications for the hydrology of the North Pacific Ocean over the past 25 kyr, *Geochemistry, Geophys.*
1013 *Geosystems*, 16(11), 3883–3904, doi:10.1002/2015GC005871, 2015.

1014 **Table captions**

1015

1016 **Table 1.** U-series ages and ϵNd values obtained for cold-water coral samples collected from sediment core RECORD 23
1017 (Sardinia Channel).

1018

1019 **Table 2.** ϵNd values obtained for cold-water corals from the southern Alboran Sea. The AMS ^{14}C ages published by Fink et
1020 al. (2013) are also reported as Median probability age (ka BP).

1021

1022 **Table 3.** AMS ^{14}C ages of samples of the planktonic foraminifer *G. bulloides* from ‘off-mound’ sediment core SU92-33. The
1023 AMS ^{14}C ages were corrected for ^{13}C and a mean reservoir age of 400 yrs, and were converted into calendar years using the
1024 INTCAL13 calibration data set (Reimer et al., 2013) and the CALIB 7.0 program (Struiver et al., 2005).

1025

1026 **Table 4.** Multiproxy data obtained for the upper 2.1 m of sediment core SU92-33 (Balearic Sea). Stable oxygen and carbon
1027 isotopes were measured on benthic (*C. pachyderma*) and planktonic (*G. bulloides*) foraminifera; ϵNd values were obtained on
1028 mixed planktonic foraminifera samples. The age results from a combination of 7 AMS- ^{14}C age measurements for the upper
1029 1.2 m of the core and by a linear interpolation between these ages as well as the $\delta^{18}\text{O}$ variations of the planktonic
1030 foraminifera *G. bulloides*.

1031

1032 **Figure captions**

1033

1034 **Figure 1.** Map of the western Mediterranean Sea showing the locations of samples investigated in this study. Yellow dot
1035 indicates the sampling location of the sediment core from the Balearic Sea (SU92-33); yellow stars indicate the locations of
1036 the CWC-bearing cores from the Sardinia Channel (RECORD 23) and the southern Alboran Sea (for further details on the
1037 CWC from the Alboran Sea refer also to Fink et al., 2013). The cores discussed in this paper (Gulf of Cádiz: IODP site
1038 U1387, Balearic Sea: MD09-2343, northern Tyrrhenian Sea: MD01-2472, Adriatic Sea: MD90-917) are indicated by black
1039 dots, and seawater stations are marked by open squares. Arrows represent the main oceanographic currents. The black line
1040 shows the general trajectory of the Modified Atlantic Water (MAW) flowing at the surface from the Atlantic Ocean toward
1041 the western and eastern Mediterranean. The orange line represents the Levantine Intermediate Water (LIW) originating from
1042 the eastern basin. The black dashed line shows the trajectory of the Western Mediterranean Deep Water (WMDW) flowing
1043 from the Gulf of Lions toward the Strait of Gibraltar.

1044

1045 **Figure 2.** (a) Sea Surface Temperature (SST) records of cores SU92-33 (red line) and MD90-917 (green line; [Siani et al.](#)
1046 [2004](#)), (b) $\delta^{18}\text{O}$ record obtained on planktonic foraminifer *G. bulloides* for core SU92-33, (c) $\delta^{18}\text{O}$ record obtained on benthic
1047 foraminifer *C. pachyderma* for core SU92-33, (d) $\delta^{13}\text{C}$ record obtained on benthic foraminifer *C. pachyderma* for core SU92-
1048 33. LGM: Last Glacial Maximum; HS1: Heinrich Stadial 1; B-A: Bølling-Allerød; YD: Younger Dryas. Black triangles
1049 indicate AMS ^{14}C age control points.

1050

1051 **Figure 3.** (a) Sea Surface Temperature (SST) record of core SU92-33 (red line), (b) ϵNd records obtained on mixed
1052 planktonic foraminifers from core SU92-33 (open circles) and from cold-water coral fragments collected in the Alboran Sea
1053 (red squares), (c) ϵNd values of cold-water corals from core RECORD 23 (Sardinia Channel).

1054
1055 **Figure 4.** (a) $\delta^{13}\text{C}$ records obtained on benthic foraminifer *C. pachyderma* for cores SU92-33 (red line) and MD99-2343
1056 (blue line; Sierro et al., 2005). (b) ϵNd records obtained on mixed planktonic foraminifers from core SU92-33 (open circles)
1057 and from cold-water coral fragments collected in the Alboran Sea (red squares). Modern ϵNd values for LIW (orange dashed
1058 line) and WMDW (blue dashed line) are also reported for comparison. (c) ϵNd values obtained for planktonic foraminifera
1059 with Fe-Mn coatings at sites 300G (36°21.532' N, 1°47.507' W; 1860 m; open dots) and 304G (36°19.873' N, 1°31.631' W;
1060 2382 m; black dots) in Alboran Sea (Jimenez-Espejo et al., 2015). (d) UP10 fraction (>10 μm) from core MD99-2343
1061 (Frigola et al., 2008). (e) Sortable silt mean grain-size of core MD01-2472 (Toucanne et al., 2012). (f) Ln Zr/Al ratio at IODP
1062 site U1387 (36°48.3' N 7°43.1' W; 559 m) (Bahr et al., 2015).

1063
1064 **Figure 5.** (a) $\delta^{18}\text{O}$ record obtained on planktonic foraminifer *G. bulloides* for core SU92-33, (b) $\delta^{13}\text{C}$ records obtained on
1065 benthic foraminifer *C. pachyderma* for core SU92-33, (c) ϵNd values of cold-water corals from core RECORD 23 (Sardinia
1066 Channel), (d) ϵNd values records obtained on mixed planktonic foraminifera from core SU92-33 (open circles) and from
1067 cold-water coral fragments collected in the Alboran Sea (red squares), (e) ϵNd values obtained on terrigenous fraction of
1068 MS27PT located close the Nile River mouth in the eastern Mediterranean basin (Revel et al., 2015).
1069

